Coordination Chemistry Reviews, 90 (1988) 243-315
Elsevier Science Publishers B.V., Amsterdam — Printed in The Netherlands

4 TITANIUM

Nick Serpone[1a], Mary A. Jamieson[1b] and E. Pelizzetti[1c].

CONTENTS

INTRODUCTION

The extent of coordination chemistry of titanium appears attenuated during 1985. By contrast, the interesting chemistry occurring in systems containing TiO_2 and related oxides continues unabated. The present review covers those papers cited in Chemical Abstracts Volume 101, No. 23 through Volume 104, No. 4. The major focus is again on titanium oxides. Several review articles have appeared that may be of interest to the readers of this work.

Nabivanets and coworkers[2] have reviewed such properties of titanium(III)

0010-8545/88/$25.55

in solutions as complex stability constants, electrical potentials, and molar absorptivities, and have further discussed these in terms of their relevance to the determination or separation of titanium. Thermal studies reported in 1983 on titanyl and zirconyl oxalate complexes have been reviewed[3], as have nmr x-ray diffraction analyses on Ti-V hydrides[4]. Reviews on (i) the physical, thermal and crystallographic character of the series Ti_nO_{2n-1}, Ti_nO, Ti_nO_{n-1}, $Ti_{n-1}O_n$ and $Ti_{2nH}O_n$ [5], (ii) the mechanism of oxidative ammonolysis of toluene on a vanadium-titanium oxide catalyst[6], and (iii) the selective thin-film treatments (e.g., TiN) for photothermal conversion of solar energy[7] have also appeared.

4.1 HYDRIDES

The semi-empirical SCF-MO-LCAO method has been used by Ivanovskii and coworkers[8] to study the electronic structure and chemical bonding in nonstoichiometric titanium (and zirconium) hydrides. The results are compared with the band structure calculations and experimental x-ray emission and photoelectron spectra. The authors also considered the influence of the concentration of hydrogen vacancies and the tetragonal distortions of the crystal lattice on the electronic energy spectrum[8].

Nuclear magnetic resonance (nmr) studies and magnetic susceptibility measurements have been reported for $Ti_{(1-x)}V_xH_2$ ($0.04 \leq x \leq 0.65$)[9] and $TiCoH_x$[10]. Entropy and enthalpy measurements on the electrochemical reaction of $TiMn_{1.5}$ hydride electrode in aqueous alkaline solution have been reported by Yayama et al.[11]. The study reveals no heat change upon hydrogenation of the electrode which occurs during the electrochemical reaction. Hydrogen evolution at potentials below -1.075V vs. Ag/AgCl under open-circuit conditions was rationalized in terms of a "local cell" model[12].

4.2 NITRIDES

The Korringa-Kohn-Rostoker(KKK)-Green function and KKK-CPA methods have been utilized to calculate the electron densities and densities of electronic states for TiN_x (x = 0.75, 1). The calculated results agree well with existing experimental evidence for vacancy-induced changes in the electronic structure of TiN[13]. Titanium nitrides of various compositions react with hydrogen at 573-1073K fo up to 100 hrs. X-ray diffraction analyses on the products show no crystal structural changes for N:Ti ratios of less that 0.3, though solid solutions of ternary compounds are formed which contain large quantities of hydrogen. Further, a body-centered tetragonal type specimen with N:Ti ≈ 0.4 transforms into a hcp-type ternary compound upon hydrogenation; the hydrogen content was twice as much as nitrogen. Upon hydrogenation, specimens of N:Ti > 0.5 yielded ternary compounds of fcc structure, wherein the amount of hydrogen absorbed was significantly less than that in ternary compounds with hcp structure[14].

4.3 PHOSPHATES

X-ray diffraction and EPR spectroscopy have been employed to determine the position of Cu in the lattice of $Cu_xNb_{1-x}Ti_{1+x}(PO_4)_3$ ($0 \leq x \leq 1$) and $Cu_{1+x}Cr_xTi_{2-x}(PO_4)_3$ ($0 \leq x < 1$), both of which have a Nascion-type structure [15]. $CuTi_2(PO_4)_3$ has been prepared, oxidized to $CuTi_4(PO_4)_6$, and characterized by x-ray crystallography [15].

High-resolution IR transmission measurements at 10-300K on $KTiOPO_4$ crystals have elucidated the hydroxide ion bands[16]. Additionally, $KTiOPO_4$ exhibits an extremely short wavelength titanate emission at 390nm, which is quenched at ≈100K. The luminescence has been discussed[17] in terms of a self-trapped exciton that gains mobility at higher temperatures.

4.4 SULFIDES

The preparation of titanium disulfides of different stoichiometries, $Ti_{(1+x)}S_2$ ($0 \leq x \leq 0.1$), has been reported; the lattice parameters have been determined. The results are discussed in terms of the addition of excess Ti to the octahedral interstices in the van der Waals gap[18]. Chemical vapor deposition from gaseous $TiCl_4$ and H_2S yields different nonstoichiometric compositions of $Ti_{(1+x)}S_2$. The excess of Ti(x) in $Ti_{(1+x)}S_2$ deceases to 0.01 as the ratio $H_2S/TiCl_4$ increases to~20. The apparent chemical diffusion coefficient of Li in $Ti_{1.01}S_2$ is 4.0×10^{-13} m^2s^{-1}[19].

Bernard et al.[20] have prepared the layered titanium dichalogenides $(NH_3)_yTiS_2$ ($0.4 \leq y \leq 0.6$) and characterized them by x-ray diffraction, vapor pressure measurements, thermogravimetric analysis, and SQUID magnetometry. The compounds rapidly lose NH_3 at ambient temeprature to form a stage II structure. The ionic formulation $(NH_4)_y,(NH_3)_y"TiS_2$ best describes these compounds, wherein the more strongly bound NH_3 is best described as NH_4^+. It appears that redox reactions play an important role in NH_3 intercalation into TiS_2, and likely into other TiX_2 hosts[20].

Structural studies on hydrated lithium intercalates of TiS_2 and $TiSe_2$[21], c-TiS_2[22], and Tl_2TiS_4[23] have appeared. Two hydrates were observed in Li-intercalated TiX_2 (X = S, Se): one contains a monolayer and the other a bilayer of water molecules between the TiS_2 layers. Structures were determined for $Li(H_2O)TiX_2$, $Li(H_2O)_2TiX_2$, $Li_{0.4}(H_2O)TiX_2$, and $Li_{0.4}(H_2O)_2TiX_2$[21]. Figure (1) shows results obtained for studies on c-TiS_2[22], while Figure (2) illustrates the crystal structure of Tl_2TiS_4. The structure of Tl_2TiS_4 has been described by Klepp[23] as a mixed packing of Tl atoms and S atoms, composed of puckered TlS_2 layers, in which the Ti atoms occupy the octahedral interstices.

The stability of the intercalated phases in Ag_xMS_2 (M = Ti, Nb, and Ta) has been elucidated by x-ray diffraction and emf measurements[24]. Extensive

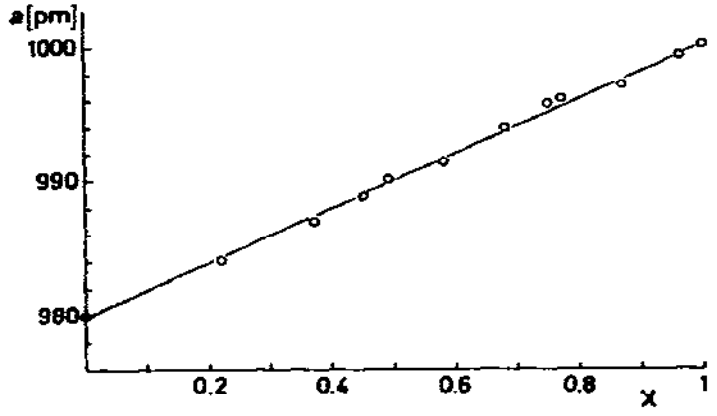

Figure 1. Variation of the cubic lattice parameter 'a' with the copper level 'x' in $Cu_xTi_2S_4$ phases prepared by anodic oxidation of the thiospinel $CuTi_2S_4$ in copper(I) electrolytes at 300K, from reference 22.

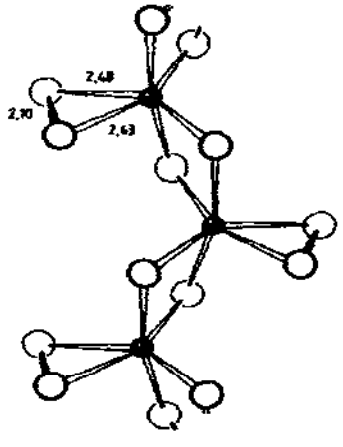

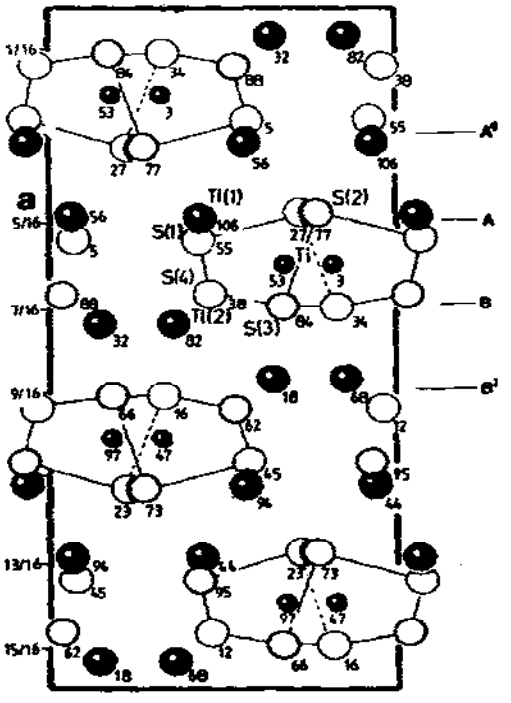

Figure 2. The (a) molecular and (b) crystallographic projection on the [001] plane of Tl_2TiS_4, from reference 23.

X-band ESR measurements on M_xTiS_2 (M = V, Cr, Mn, Fe, Co, Ni; $0 \leq x \leq 1$) at 300 - 77K have shown variations in the intra- and inter-layer spacings upon intercalation of guest atoms. While Fe_xTiS_2 and Ni_xTiS_2 show no ESR signals and magnetic interactions are ineffective in V_xTiS_2, dipolar interactions appear dominant in Cr_xTiS_2 and Mn_xTiS_2 [25].

4.5 HALIDES

Choudhury and coworkers[26 - 30] report extensive studies on phase transitions in manganese and zinc fluorotitanate compounds. Raman spectra of $MnTiF_6 \cdot 6H_2O$, $MnTiF_6 \cdot 6D_2O$, $ZnTiF_6 \cdot 6H_2O$ and $ZnTiF_6 \cdot 6D_2O$ single crystals were studied under different polarizations in the temperature range 77 - 300K. The observed bands are assigned to the various vibrational modes[26 - 28]. A Raman study of $MnTiF_6 \cdot 6D_2O$ reveals a structural phase transition between 200 and 228K, and asymmetry in the shape of the spectrum at 220 - 360cm^{-1}. The asymmetry arises from coupling between the ν_{as}(Mn-O) and $\delta(TiF_6)$ modes present in this region[27]. Additionally, it seems that for the frequency shift, the quartic interactions, quadratic in the soft mode coordinates, are important; for the linewidth, the pure vibrational dephasing (elastic scattering) process is important[29]. Infrared spectra of $ZnTiF_6 \cdot 6H_2O$ and $MnTiF_6 \cdot 6H_2O$ were obtained in the temperature range 166 - 300K [30]. Two vibrational modes (at 435 and 485cm^{-1}) appear below 185K in the spectrum of $ZnTiF_6 \cdot 6H_2O$; whereas above T_c = 203K, only one vibrational mode is present. The spectrum of $MnTiF_6 \cdot 6H_2O$ shows two vibrational modes (at 440 and 485cm^{-1}) below 169K, and one vibrational mode above T_c = 254K [30]. The temperature dependence (77 - 400K) study of the nmr linewidths of ^1H and ^{19}F in $NiTiF_6 \cdot 6H_2O$ shows separate abrupt changes in the ^1H width (122 - 126K) and the ^{19}F width (131 - 134K). The data confirm the existence of two transitions in the known structural transformation region. An anomaly near 205K suggests the possibility of a third transition. Cheung and Lichti[31] have discussed this temperature dependence in terms of

reorientations of the octahedral complex ions.

Reaction of TiO_2 in 40% HF with an excess of 30% H_2O_2 and KOH, followed by the addition of aqueous HF to adjust the solution pH, results in the formation of $K[Ti(O_2)F_3]\cdot H_2O$, with the peroxide bonded to the Ti(IV) center in a triangular bidentate manner (C_{2v}). The product was characterized by infrared and laser Raman spectroscopies[32]. K_2TiOF_4 has been prepared *via* three methods[33]: (a) solid state reaction between K_2TiF_6, TiO_2 and KF; (b) pyrohydrolysis of K_2TiF_6 at 723 and 823K; and (c) thermal decomposition of $K_2Ti(O_2)F_4\cdot H_2O$. In all three methods, the reaction products are mixtures of several compounds, including the kryolith-phase $K_{2+x}TiO_xF_{6-x}$ and TiO_2. At 403K, $K_2Ti(O_2)F_4\cdot H_2O$ forms $K_2Ti(O_2)F_4$ *via* loss of H_2O, and at 503K the peroxo group decomposes to yield K_2TiOF_4 as the main product. K_2TiOF_4 crystallizes tetragonally; an analysis if its infrared spectrum suggests infinite ~Ti-O-Ti-O- chains[33].

The infrared spectrum of TiF_4, consisting of a single band at 772cm^{-1}, was recorded on the products of the reaction between $TiCl_4$ and NaF at 900 - 1200K. The band at 772cm^{-1} is due to the ν_3 stretching vibration[34]. The Raman spectrum of the trigonal $[(NH_4)_2TiF_6]$ complex in the temperature range 10 - 298K confirms the presence of four modes, as predicted by group theory. Tentative assignments are reported by Jenkins[35].

A review by Galitskii *et al.*[36] discusses the preparation of high-purity $TiCl_4$ by chlorination of synthetic titanates. The formation and structures of $RbTiCl_3$ and $CsTiCl_3$ in RbCl-Ti-$TiCl_3$ and CsCl-Ti-$TiCl_3$ systems has been reported[37]; they are isotopic with the structure of $CsNiCl_3$, with space group $P6_3/mmc$. The preparation, characterization and solution properties of $MgCl_2\cdot TiCl_4\cdot 4L$ (L = EtOAc, THF, HCO_2Et), $MgCl_2\cdot TiCl_4\cdot 2EtOAc\cdot 2L$ (L = HCO_2Et, BzOEt), $MgCl_2\cdot TiCl_4\cdot 2EtOAc$ and $(MgCl_2)_3\cdot TiCl_4\cdot (SnCl_4)_2\cdot 12EtOAc$ have been investigated[38]. The $TiCl_6^{4-}$ and $TiCl_6^{3-}$ species were identified by electronic spectra from solutions of $TiCl_2$ and $TiCl_3$ in NaCl-KCl melts. By contrast, $TiCl_2$ and $TiCl_3$ in KCl-NaCl-NaF melts form $TiCl_3F_3^{3-}$ and $TiCl_2F_4^{3-}$ [39].

The energy terms and partial charge densities of core-excited states have been estimated for MCl_4 (M = Ti, Si, C) by SCF-X_α scattered-wave calculations and a muffin-tin approximation. The results are in good agreement with data obtained from x-ray absorption and electron energy-loss spectra. The absorption edge of $TiCl_4$ is dominated by antibonding $\underline{d}(e)$ and $\underline{d}(t_2)$ orbitals [40]. Following a vibrational analysis on $\underline{trans}$-$[TiCl_2(H_2O)_4]^+$, molecular constants, force constants, compliance constants and centrifugal distortion constants were evaluated using the kinetic constants method[41].

High-precision calorimetry has been employed to determine the heats of reaction leading to the formation of complexes from reaction of $TiCl_4$ with ethyl acetate, acetone or methylethylketone in benzene solutions. The reactions involve three stages, with formation of 1:1 and 1:2 complexes together with dissociation of the acceptor complex formed first with the initial solution[42]. $TiCl_4 \cdot 2CH_3CN$ is obtained $\underline{via}$ interaction of the components, followed by crystallization from acetonitrile. X-ray diffraction studies show monoclinic crystals, space group $P2_1/c$, with "a" 5.982(8), "b" 13.50(2) and "c" 13.15(2)Å, and the two N atoms $\underline{cis}$ to each other[43,44]. Magnesium reduces $TiCl_4(THF)_2$ in THF under nitrogen to $TiNMg_2Cl_2(THF)$; this species reacts further with CO to yield $TiCONMg_2Cl_2(THF)$. The amide character of N in $TiNMg_2Cl_2(THF)$ is suggested by the reaction between $TiCONMg_2Cl_2(THF)$ and MeI to give Me_2NCOMe in 73% yield. The following reactions were also studied[45].

$$TiNMg_2Cl_2(THF) + I_2 \longrightarrow TiNMgCl(THF)$$

$$\downarrow +CO \qquad \{1\}$$

$$Ti(NCO)MgCl(THF)$$

The kinetics and mechanism of the chemisorption and reaction of $TiCl_4$ with copper films were studied gravimetrically by Dobruskin and coworkers[46]. The reaction is catalysed by oxygen. In an effort to improve the efficiency of

magnesium consumption in the manufacture of titanium sponge, the mechanism of reduction of titanium chlorides by magnesium was investigated in a salt melt (34.6% $TiCl_2$, 19.1% $TiCl_3$, 21.1% NaCl, 25.2% KCl)[47].

The hydrolysis of titanium(IV) in chloride media has been studied by determining the [Ti(IV)]/[Ti(III)] ratios in solutions of $TiCl_4$ equilibrated with hydrogen gas at 298K in 3M (Na)Cl; the $Ti(OH)_2^{2+}$ species predominates in the concentration ranges $0.5 \leq [H^+] \leq 2M$ and $1.5 \times 10^{-3} \leq [Ti(IV)] \leq 0.05M$. Reduction potentials were evaluated from equilibrium data, and as a function of $[H^+]$ [48]. The nature of Ti(III) in absolute ethanol in the presence of HCl has been established from electronic and ESR spectra. The ESR signals were assigned to the species $[TiCl_{6-n}(EtOH)_n]^{3-n}$ (n = 1, 2, 3, 4); the complexes with n = 2, 4 have cis structures. Only $TiCl_3(EtOH)_3$ obtained in the absence of HCl[49].

$TiCl_4$ reacts with 2-pyridylphenylacetonitrile (L) and 1,2-dicyano-1,2-di(phenyl)-1,2-(2-pyridyl)ethane (L') in 1,2-dichloroethane or ether to yield $TiCl_4L$ and $(TiCl_4)_2L'$, respectively[50]. Chelation, metal uptake and distribution ratio of $OC[N(CH_2O_2CC_6H_4OH\text{-}\sigma)_2]_2$ with $TiCl_4$ are reported by Siddiqi and coworkers[51]. The resulting complexes were characterized by elemental analyses, infrare spectroscopy and molar conductance. The preparation of TiL_2 (H_2L = rubeanic acid) from $TiCl_4$ and H_2L has been reported, along with proposals for monomeric and polymeric structures of TiL_2[52].

Catalyst complexes have been prepared from $TiCl_4$. Polystyrene cross-linked with 5-7% divinylbenzene and combined with $TiCl_4$ in CS_2 forms a stable complex containing 4.5% Cl capable of catalysing the conversion of aromatic aldehydes, carboxylic acids, ketones and some alcohols into the corresponding acetals, esters, ketals and ethers, respectively. The complex is also effective for the Friedel-Crafts alkylation reaction[53]. Reaction of $TiCl_4$ with EtOH, PrOH (or other alcohols) or lithium alcoholate in an organic solvent in the presence of a NH_4NO_3, NH_4I, or NH_4CNS solution in liquid NH_3 or in the presence of an organic amide affords alkyl ortho-titanates. These complexes can catalyse polyester synthesis and epoxy resin curing[54]. Aromatic ketones react

smoothly in basic media in the presence of $TiCl_3$ to give reductively coupled products according to the increase of reducing power of the Ti(III) ion with increasing pH. Thus, benzil, benzoin and methoxybenzoin are reduced to the corresponding alcohols[55]. The reduction of the acyclic diketone $MeCOCMe_2COMe$ by different hydrides in several solvents yields the (±)- and meso-diol; the (±)-diol predominates in most cases. By contrast, the meso-diol is favored in the presence of $TiCl_4$. A cyclic model is suggested to account for the induction phenomena observed[56]. Alkenyl sulfides can be reduced to the corresponding alkyl sulfides with Et_3SiH in the presence of $TiCl_4$. The reduction apparently proceeds via (phenylthio)alkyltitanium intermediates[57].

The treatment of the cyclopropanecarboxylate derivatives (1) and (2) with PhSeCl in CH_2Cl_2 in the presence of $TiCl_4$ yields $RCOCMe_2CH(SePh)CO_2Me$ (R = H, Me), and $Me_3CCOCR'(SePh)CO_2Me$ (R' = H, Me), respectively. Similarly, the

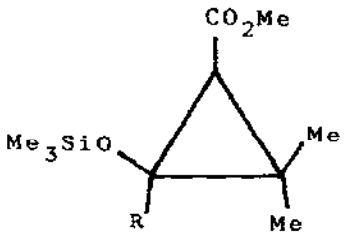

(1)

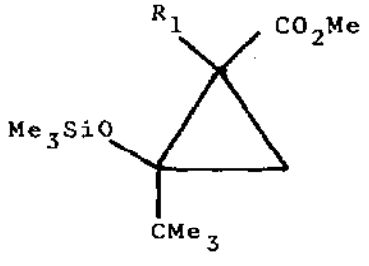

(2)

synthesis of $Me_3COCH_2CH(CO_2Me)SC_6H_4$-$NO_2$-m is given. $TiCl_4$ promotes the ring cleaving reaction[58]. Titanium tetrachloride induces the functionalization of the dibenzodiazocinedione (3). Upon reaction of (3) with 1-methylpiperazine, $TiCl_4$, and PhOMe, the dibenzodiazocine (4) (NR_2 = 4-methyl-1-piperazinyl; R_1 = H) obtains[59].

Bikushev[60] has investigated the activity of catalytic systems composed of an alkylaluminum halide, $TiCl_3$, and a phosphonate in the stereospecific polymerization of propylene. Chemical and kinetic methods were employed to

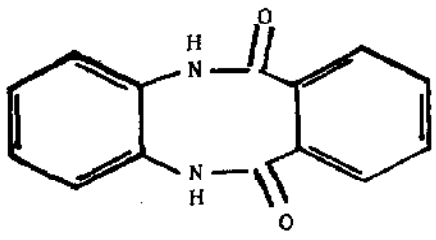

(3)

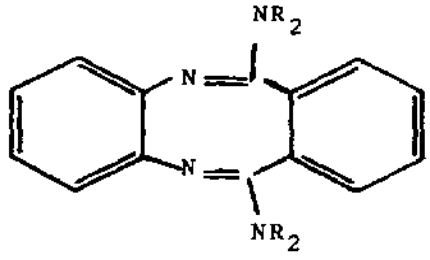

(4)

demonstrate the disproportionaltion of the alkylaluminum halides in the presence of a phosphonate and formation of new catalytic complexes. Spectroscopic analyses (XPS, ir, nmr) and solvent extraction methods have confirmed that $TiCl_4 \cdot 2Et_2O$ reacts with the $3TiCl_3 \cdot AlCl_3$ catalyst in the solid state (reaction 2). The surface structure of the catalyst is described by a three-layer model [61]. EPR spectroscopy was used to study the reactions in the catalytic system

$$TiCl_4 \cdot 2Et_2O + 2\ AlCl_3 \longrightarrow 2\ AlCl_3 \cdot Et_2O + TiCl_4 \qquad \{2\}$$

$TiCl_4$--PhCOMe—$Al(Bu^i)_3$ as a function of their relative concentration effects. Six types of bi- and tri-nuclear paramagnetic Ti^{3+} centers are formed in the system; those containing PhCOMe are stable compared to Ti^{3+} complexes which have no electron-donor ligands[62]. Thekinetics of the surface photochemistry in adsorbed mixtures of $TiCl_4$ and $Al_2(CH_3)_6$ have been studied by UV-laser-induced photodeposition. In addition to the individual adsorbed-phase photoreactions of $TiCl_4$ and $Al_2(CH_3)_6$, a new photoreaction channel was observed in the presence of

both. The new channel is ascribed to a two-component photoreaction in the adsorbed mixture, as deduced from pressure dependency studies of the reaction rate. The data could be qualitatively understood in terms of a Langmuir-Hinshelwood mechanism in conjunction with competitive adsorption of $TiCl_4$ and $Al_2(CH_3)_6$ [63].

The selective methylation of homo-propargyl alcohols to give alkenols, after hydrolysis, is catalysed by $TiCl_4$--$AlMe_3$ in CH_2Cl_2. The alkenols $HOCHRCH_2CH{=}CR'Me$ (R = H, Me, Et; R' = H, Me, Et, Pr, Me_2CH, Bu, pentyl, Ph) have been obtained[64]. The oligomerization of propene in the presence of Co_2O_3--$TiCl_4$--Et_2AlCl gives predominantly 4-methylpentenes. Similar oligomerization in the presence of NiO--$TiCl_4$--Et_2AlCl yields maninly 2-methylpentenes and dimethylbutenes[65].

A kinetic study on propylene polymerization in the presence of the catalyst system composed of $MgCl_2$--supported $TiCl_4$ with Et_3Al and ethyl benzoate (EtOBz) was undertaken by Kashiwa and Yoshitake[66] to elucidate the role of EtOBz, known to increase stereospecificity of the product. It seems that EtOBz modifies the isotactic specific centers so as to increase the k_p(isotactic) value. As a result, the productivity and molecular weight of the isotactic polymer are increased[66]. Spitz and coworkers[67, 68] have carefully examined the precatalyst system $MgCl_2$--$TiCl_4$--aromatic ester for propene polymerization. There was found to be (a) a continuous decrease in the polymerization rate during polymerization, characterized by a deactivation index not dependent on the precatalyst but on the cocatalyst; (b) isotacticity control by the [Al]/[aromatic ester] ratio in the cocatalytic solution; and (c) fast and reversible control of kinetics and tacticity by the [Al]/[aromatic ester] ratio. Infrared studies suggest that the role of the electron donor is to (i) control the fixation of $TiCl_4$ on $MgCl_2$in the precatalyst; and (ii) regulate the isospecificity of the active site by contact with the alkylaluminum-aromatic ester complex; and (iii) slows polymerization in the cocatalytic solution[67]. The pressure dependence of propene polymerization

under these conditions reveals an immediate onset of polymerization after C_3H_6 introduction at approx. 333K [68]. Kashiwa and coworkers[69, 70] investigated the copolymerization of ethylene with propylene in the presence of a $MgCl_2$--$TiCl_4$--Et_3Al--EtOBz catalyst system, as well as a catalyst system composed of $MgCl_2$--$TiCl_4$--$AlEt_2Cl$--2-ethoxyethanol/n-decane. Both catalyst systems exhibit very high activity relative to the conventional $TiCl_3$--$AlEt_2Cl$ system. However, the two catalyst systems do differ with respect to the microstructure of the copolymer product. Specifically, the $MgCl_2$—$TiCl_4$--$AlEt_2Cl$--2-ethoxyethanol/ n-decane system brings about more random distribution of the monomeric units and also decreases regiospecificity with regard to the arrangement of the propylene unit[69]. The copolymerization of ethylene with α-olefins (propylene, butene-1,4-methyl-1-pentene) catalysed by $MgCl_2$--supported $TiCl_4$ combined with Et_3Al at temperatures $\leq$443K is homogeneous. Of the three types of co-monomers, propylene exhibits the highest reactivity, most frequently causes the termination of a polymer growing *via* chain transfer reaction, and produces copolymers having the broadest molecular weight distribution[70].

X-ray diffraction and thermal analysis were employed to examine the polymorphism of TiI_4. A cubic phase transition occurs at 387K to a triclinic crystal. A second triclinic modification takes place on treating the first one *in vacuo*[71]. Reaction between TiI_4 and CsI affords Cs_2TiI_6; thermal stabilities are reported[72].

4.6 OXIDES, TiO_x and TiO_2

The stability and interaction of crystallographic shear planes in TiO_{2-x} (rutile) have been examined by theoretical methods[73]. The model predicts that the nonstoichiometry can largely be accomodated by crystallographic shear planes which interact to form arrays. The model also reproduces the various structural features found for this material.

The interaction of SO_2, CO, H_2O and O_2 with the nearly perfect $(10\bar{1}2)$

surface of corundum Ti_2O_3 has been investigated[74]. SO_2 adsorbs dissociatevily onto Ti_2O_3, and catalyses the complete oxidation of the surface to TiO_2 and TiS_2. The reaction is accompanied by large-scale surface disorder and by an increase in the work function. The chemisorption mechanism of CO is tentatively identified as dissociative adsorption at defect sites.

Hydrated oxides of titanium and antimony were prepared by simultaneous precipitation of $TiCl_4$, $SbCl_5$ or $SbCl_3$ by NH_4OH at pH 7 and 343K. The specific surface area of the oxide hydrates decreases as the Sb^{3+} or Sb^{5+} oxide hydrate concentration increases. On aging, the specific surface area passes through a maximum at 7-10 mol% Sb_2O_x, then decreases to a minimum at 50-70 mol% Sb_2O_5, and then increases. The results are explained in terms of phase composition changes[75].

In the Russian literature there are two articles of interest: (1) a thermodynamic study of the high-temperature reduction of titanium, zirconium, molybdenum and tungsten oxides in nitrogen[76], and (2) a study of the effects of titanium and calcium oxides on the activity of an ammonia synthesis catalyst on an iron-aluminum borate support[77].

Harada and coworkers[78] prepared TiO_2 from aqueous $TiCl_4$ by three different methods: (a) neutralization with a 14% NH_4OH solution; (b) hydrolysis in water at >353K; and (c) hydrolysis in a 0.5N HCl solution. X-ray diffraction and thermal analyses of the resulting TiO_2 reveal that the degree of crystallization and photocatalytic activity increase in the order (a) < (b) < (c). TiO_2 has also been prepared from $TiCl_4$ or $Ti(Pr^iO)_4$, and its nature investigated by thermal analysis, x-ray diffraction, measurements of specific area and catalytic activity for CO oxidation. The polymorphic form of the TiO_2 prepared from $TiCl_4$ changes from anatase to rutile at 923-1173K; this temperature is significantly higher than that for the same compound from $Ti(Pr^iO)_4$. The catalytic activity of the TiO_2 prepared from $TiCl_4$ is greater than 3-fold as high as that of the TiO_2 from $Ti(Pr^iO)_4$ in the CO oxidation reaction[79]. Moreover, TiO_2 catalysts prepared[80] from $Ti(Pr^iO)_4$ can be

modified in terms of surface and internal electronic structure by the preparative method employed. The hydrolysis of $Ti(Pr^iO)_4$ followed by calcination at temperatures $\leq$1273K yields TiO_2. Upon an increase in the calcination temperature up to 823K, there is an increase in anatase content and crystallite size. At 823-873K, a mixture of anatase and rutile obtains; while at higher temperatures, only rutile is obtained[81]. The photocatalytic activity of these TiO_2 powders was examined in aqueous isopropanol, aqueous Ag_2SO_4, and aqueous Ag_2SO_4 containing isopropanol. Abrahams et al.[82] report that an increased photocatalytic activity is obtained in the decomposition of H_2O, acetic acid and propan-2-ol when the x-ray amorphous TiO_2 is heated at 623K for 1-4 hrs.

TiO_2 incorporated into Nafion or clay films was prepared via treatment of the TiO_2 with Ti(III) followed by oxidation. ESR spectroscopy has characterized the state and chemical reactivity of the titanium species in Nafion. Both systems exhibit photocatalytic activity in the reduction of methylviologen with oxidation of triethanolamine[83].

Electronic absorption spectroscopy of 4-dimethylaminoazobenzene adsorbed onto TiO_2(anatase) has been used to identify OH groups remaining on the surface after thermovacuum pretreatment. The observed behavior was explained in terms of the change in Ti^{3+} surface concentration with temperature[84]. Busca et al. [85] have examined the interaction of methanol with pure and KOH-doped TiO_2(anatase) using TPD, FT-ir and catalytic studies. The results indicated a number of hydrogen-bonded and chemisorbed species on the TiO_2 surface. KOH poisons the Lewis and Broensted acid sites of TiO_2. Further, the methoxy groups on $TiO_2$are formed by several mechanisms, including: (a) methanol dissociation on acid-base pairs, (b) reaction of methanol with surface OH groups, and (c) possibly decomposition of chemisorbed species[85].

The influence of temperature and chlorine contamination on the surface area and morphology of TiO_2(anatase) was examined in connection with typical catalyst preparation and reactions conditions. Adsorption, wide-angle x-ray diffraction

and SEM techniques show that chlorinated samples have lower surface areas and exhibit lower resistance to sintering than does blank TiO_2[86]. High-resolution electron microscopy was used to determine the fine structure of extended defects occurring within samples of mechanically deformed and reduced TiO_2(rutile), $\simeq TiO_{1.9966}$ [87]. The stoichiometry dependence of the dissolution temperature and the phase limits of nonstoichiometric TiO_{2-x} (x = 1.9966, 1.9979, 1.9986) were established by in situ transmission electron microscopy (TEM). The defect structure formed during dissolution and the reprecipitation of extended defects upon cooling have also been studied[88]. Crackel and Struve[89] have verified dye-to-surface nonradiative excitation transfer as an important decay mode for S_1 state cresyl violet separated from a TiO_2 surface by 80 - 509Å.

ESR spectra of TiO_2 containing copper(II) impurity ions subsequent to mechanical activation reveals that Cu(II) is stabilized in octahedral and square pyramidal sites of the TiO_2 lattice. Mechanical activation of anatase gives the rutile phase[90]. Samples of the ternary CuO--TiO_2--Sb_2O_5 system were investigated by ESR, x-ray phase and structural analyses. A solid solution with rutile structure is formed for 0.07/0.93/0.0012-0.13 $Sb_2O_5/TiO_2/CuO$, in which Sb is pentavalent and the isolated Cu ions and their associates are located at nodal sites in the rutile lattice[91].

Graetzel and Rotzinger[92] have examined the influence of crystal lattice structures of TiO_2 and $SrTiO_3$ on the conduction band energy. EHMO calculations on model complexes show that the energy levels of the LUMO's involving predominantly the 3dπ orbitals xy, xz and yz, and of titanium, are sensitive to the lattice structure. A Raman spectroscopic study of TiO_2 coatings shows that upon laser annealing, the amorphous coatings are transformed into microcrystals of anatase structure at lower laser intensities, and a mixture of anatase and rutile structures at higher intensities[93]. The experimental determination of the total light distribution in an aqueous solution of TiO_2 for an almost non-absorbing wavelength reveals that the extinction coefficient exhibits a

non-linear dependence on the concentration at high solute concentrations[94].

Thermogravimetry has established the nature of the intrinsic and extrinsic defects in TiO_2 and NbO_2, as determined for $Nb_yTi_{1-y}O_{2\pm x}$ solid solutions[95]. Pure TiO_2 is an oxygen-deficient oxide, while NbO_2 is a metal-deficient oxide. The main defects in TiO_2 are oxygen vacancies, doubly ionized $V_O^{\cdot\cdot}$ or singly ionized $V_O^{\cdot}$, and interstitial $Ti_i 3$. The nature of intrinsic defects in TiO_2 are Schottky defects. The surface acidity of four different anatase preparations was studied by FT-ir spectroscopy of adsorbed benzene, ammonia, pyridine, carbon monoxide and carbon dioxide. The surface chemistry depends on the preparation method. Pure anatase does no exhibit Broensted acidity; however, SiO_2 or sulfate impurities in the TiO_2 cause a significant enhancement of Broensted acidity[96]. Babuji and Radhakrishna[97] observed that the UV-visible transmittance of TiO_2 thin films on a glass substrate decreases on increasing the film thickness from 65 to 160nm. The spectra suggest the existence of an absorption edge in the UV region.

Temperature-programmed desorption (TPD) of CO, H_2, CO_2 and H_2O has probed the adsorptive properties of TiO_2 surfaces with different oxidation states[98]. The oxidation state, varying from Ti^{4+} to Ti^{2+}, can be altered <u>via</u> vacuum annealing of an oxidized Ti foil at 573 - 1073K. Carbon monoxide is weakly adsorbed in a carbonyl fashion on coordinatively unsaturated cation sites, while CO_2 adsorbs in a linear molecular fashion at exposed cation sites or as monodentate carbonates at surface oxygen anions. Titania surfaces are inert to H_2 adsorption and dissociation. Water adsorbed both molecularly and dissociatively, with molecular hydrogen evolution becoming more extensive on surfaces which were initially more reduced. The results of this investigation have been discussed in terms of the role of TiO_2 oxidation state in CO hydrogenation over TiO_2-supported metal catalysts[98]. An infrared study of $^{12}C^{16}O$ and $^{13}C^{16}O$ adsorbed at 77K on ZnO, TiO_2, BeO, Al_2O_3 and SiO_2 provides details on two kinds of interactions between the adsrobed molecules[99]. One interaction is chemical in nature, involving the weakening of the electron-donating ability of the metal ion after occupation of the adjacent sites with

adsorbed molecules. The second type of interaction is dipole coupling.

Studies of chenges in hydrated TiO_2 during heat treatment have been reported. During thermal treatment at 293 - 673K and 773 - 973K of $TiO_2 \cdot 0.53H_2O \cdot 0.05SO_3$, dehydration and desulfatization, respectively, occur. These processes are accompanied by the generation of active centers on the TiO_2 crystal surface, resulting in a change in the light absorption coefficient[100]. The same authors[101] report on the changes in the proton structure of hydrated TiO_2 during thermal treatment. Hydrated titania, prepared by thermal hydrolysis of H_2SO_4 solutions of titanium(IV) sulfate compounds, was investigated with respect to structure and state of protons during aging in air and heat treatment[102].

Thin-film TiO_2 prepared by sputtering methods under certain specified conditions exhibits single-crystal rutile behavior. Quantum efficiencies are comparable for all samples, and linear Mott-Schottky plots obtained with little frequency dispersion for suitable doping densities[103]. Anodization of unalloyed titanium (T40) in different electrolytes (H_2SO_4 and Na_2SiO_3) was performed to determine the amount of foreign ions incorporated into the oxide layers during the film growth. The resulting anodic oxide films were characterized by nuclear microanalysis, electron spectroscopy and glow discharge spectroscopy[104].

TiO_2 photoanodes have also been prepared by the plasma spray technique on titanium, graphite and Al_2O_3 substrates. Electrochemical and photo-electrochemical characteristics of these systems are reported for oxygen-saturated solutions of sodium hydroxide at pH 13 [105]. The electrode performance is insensitive to the plasma power and TiO_2 powder granulation; it is dependent on the purity of the spraying material, to the substrate and to the nature of the heat treatment. Zarks et al. [106] report characteristic changes in the process of formation of a crystalline phase of hydrated TiO_2, specifically the dielectric characteristics, electrical conductivity and features of the paramagnetic centers. These processes are caused by a growth

of a crystalline phase, by the anatase-to-rutile transition, by the complex chemical composition of the sample, and by the inclusion in the composition of solid particles[106].

Roy and coworkers[107, 108] have utilized a modification of the photocurrent onset potential method to obtain a flat-band potential, V_{fb}, value for TiO_2 in 0.1M NaOH. A more reliable V_{fb} value is obtained by illuminating the semiconductor with high-frequency chopped light during the potential scan, with a rate significantly slower than the chopping frequency of the light source. The potential increase of vacuum-treated TiO_2(anatase) dispersed in 1M $HClO_4$ with or without formic acid has been measured under illumination using an In_2O_3 probe[108]. The following observations were made: (a) The TiO_2 particles have an electron potential 240 meV higher than that of the Fermi level of n-TiO_2 crystal under illumination in the absence of formic acid; (b) Upon the addition of formic acid, the potential increases by 173meV, a value high enough to reduce water in the presence of a suitable catalyst. A photoelectrochemical method is reported by Jarrett[110] to measure the density of states at a TiO_2/electrolyte surface. Additionally, the Schottky barrier height for several redox couples was obtained for the surface containing this measured density. Photocurrent and photovoltage transients at n-TiO_2/electrolyte junctions have been measured using nanosecond-laser pulse excitation. Two different types of build-up were observed, both independent of excitation intensity and external resistance[111].

Electrochemical and photoelectrochemical methods have characterized colloidal TiO_2 particles at the optical rotating disk electrode (ORDE)[112]. The electron-transfer reactions between the particles and the electrode are irreversible, while the kinetics of the system obey both the Tafel and Levich relations. Other parameters determined included (a) quantum efficiencies for the photogeneration of majority carriers, (b) the number of electrons in the conduction band, and (c) their quantum efficiency and lifetime[112]. Coulostatic pulse relaxation experiments have been performed on some colloid

chemical aspects of the oxidized titanium/electrolyte interface. An analysis of the experimental results, calculations and known models has led Smit[113] to a modified colloid chemical site dissociation site binding model, having low values for the Helmholtz layer capacitance and at least two parallel impedance branches on the electrolyte side. A TiO_2 membrane cell was devised by Yonezawa et al.[114] to study the photoelectrochemical processes at a TiO_2/aqueous solution interface. Photocurrent measurements would seem to suggest that the electrons and holes generated in TiO_2 with band-gap irradiation produce reduction at the dark side and oxidation at the illuminated side of the TiO_2 membrane, respectively.

The behavior of thin metal layers of gold present on n-TiO_2 electrodes cannot be explained by the conventional potential barrier model for metal-semiconductor contacts[115]. However, it seems that the discontinuous structure of the metal layer is responsible for the anomalous photovoltaic effect. Doping thin-film polycrystalline n-TiO_2 photoanodes with such elements as Al, Y, Cr, Fe, Zn, Cd, La, Nd, Ce, La-Cr and Y-Cr has been reported[116]. Simultaneous doping with Y-Cr or La-Cr not only enhances the quantum efficiency of the photoanode, but also extends its spectral response to visible light. The latter effect is attributed to the formation of a d band[116]. The photoelectrochemical behavior of a ruthenium-doped TiO_2 crystalline electrode ($Ti_{0.97}Ru_{0.03}O_2$) reveals (a) sensitization to visible light, and (b) reduction of the overpotential for oxygen evolution, both in the dark and under illumination[117]. The $Ru^{4+} \rightarrow Ti^{4+}$ electronic transition is responsible for the subbandgap photoresponse. Furthermore, the semiconductor surface becomes positively charged under positive polarization of the electrode, and the Fermi level is pinned, facilitating charge transfer from the filled levels of water molecules to the semiconductor conduction band, therein leading to oxygen evolution.

Viehbeck and DeBarry[118] have studied the electrochemistry of Prussian blue films on spark anodized n-TiO_2 electrodes, and report evidence for four

redox states for Prussian blue. Moreover, they discuss the photoelectronchromic behavior of this system[118]. Photoelectrolysis in an electrolyte containing water soluble aromatic compounds affords the formation of hydrophobic organic layers on the TiO_2 surface. The reaction yields a hydrophilic and hydrophobic pattern on the electrode surface. The phenol/TiO_2 system has been studied in detail[119].

Anton ucci and coworkers[120] have shown the mechnaism of oxygen evolution on TiO_2 photoanodes by relating structural properties and electrochemical properties to the performance of photoelectrochemical cells of five specimens of lowest and highest photoelectrochemical efficiency. The mechanism of the discharge-ionization of hydrogen on a TiO_2(rutile) surface, as well as solid solutions based on it, have been discussed[121]. A simplified method of fixing a titanium oxide redox system onto the surface of a titanium cathode, as well as details on the reduction of nitrobenzene on these cathodes have been reported by Beck and Gabriel[122].

Nonmetallized TiO_2 powder incorporated into a thin, porous layer above a metallized substrate photosensitizes the decompositions of water and acetic acid in an aqueous gas-phase environment. Quantum efficiency values suggest that this structure has a catalytic activity comparable to dispersions of partially metallized powders[123]. Serwicka[124] has examined the interaction of water vapor with polycrystalline TiO_2(anatase) by ESR techniques at room temperature and 77K. The results suggest a photocatalytic decomposition of the water vapor at the TiO_2 surface.

In order to convert solar energy <u>via</u> decomposition of water, the formulation of a corrosion-resistant semiconductor anode materal sensitive to the visible spectral range is a prerequisite. As such, a system has been examined that consists of a heterostructure of a relatively narrow-band semiconductor (GaAs) and a protective coating based on a corrosion-resistant wide-band semiconductor (TiO_2)[125]. Another suggested route is to chemically process an oxide (TiO_2, ZrO_2, HfO_2, $SrTiO_3$, Sr_2TiO_4, $SrZrO_3$, $Sr_3Zr_2O_7$, KTi_6O_{13},

$BaTiO_3$) by cycling in CS_2 and oxygen, followed by combination with platinum or nickel. Visible light illumination of TiO_2(anatase) generates hydrogen from a 1:1 H_2O/Pr^iOH system[126]. Inoue and coworkers[127] have observed enhanced photocatalytic activity on depositing a thin TiO_2 film on ferroelectric substrates having a polarization vector. The ferroelectrics were (a) a $LiNbO_3$ single crystal with a polarization vector perpendicular to the surface; (b) a $LiTaO_3$ single crystal with the polarization vector parallel to the surface; and (c) α-Al_2O_3 single crystal for comparative purposes. From the TiO_2-thickness dependence upon hydrogen evolution from water decomposition, it was shown that the ferroelectric polarization field works to enhance the photocatalytic activity of the combined semiconducting TiO_2 films, particularly for the perpendicular polarization[127].

Salvador[128,129] and Decker[128] have examined the generation of hydrogen peroxide during water photoelectrolysis at n-TiO_2 using a rotating ring-disk electrode (RRDE). Mechanisms describing oxygen evolution *via* the photogeneration of H_2O_2, which are consistent with the observed results at the RRDE, were postulated[128]. A kinetic model based on the photogeneration of surface species, intermediates of the oxygen evolution reaction, has allowed a quantitative explanation for the main transient features observed as a function of semiconductor band bending and photon flux. Two parallel mechanisms are believed to be involved in this model: i) a time-dependent cathodic back reaction of photogenerated surface intermediates with conduction band electrons, opposite to the anodic photocurrent; and ii) a band-bending modulation due to the accumulation of positive charge at the semiconductor surface produced by hole trapping at active OH^- surface groups[129]. Rives-Arnau[130] has published a polemic in response to a paper by Muraki *et al.*[131] on the photocatalytic oxidation of water to hydrogen peroxide by irradiation of aqueous TiO_2 suspensions.

The rotating ring-disk technique has been employed to study the competition between the oxidation of H_2O and that of Br^- at an illuminated TiO_2(rutile)

anode. The study was performed as a function of the Br^- concentration at the surface, the light intensity, the electrode potential, and the surface pretreatment. A mechanism is proposed[132].

Kalyanasundaram and Graetzel[133] have studied the efficiency and long-term stability of colloidal and high surface-area powdered TiO_2 as mediators in the light-induced cleavage of water to hydrogen and oxygen, and the cleavage of H_2S to hydrogen and sulfur. Specifically, they investigated the charge transfer phenomena occurring at the TiO_2/solution interface, new methods of dispersing highly active catalysts on the TiO_2 surface, and overall light-to-chemical energy conversion efficiencies in the water cleavage reaction. The quantum yields of hydrogen production have been optimized as a function of pH, component concentration and nature of photocatalyst in the $Ru(bpy)_3^{2+}$ (bpy = 2,2'-bipyridine)/methylviologen/EDTA/catalyst system[134]. Of the various heterogeneous catalysts studied, Pt was the most efficient of the supported (on TiO_2) metals. Optically and polarigraphically measured initial photo-reduction rates of methylviologen on polycrystalline TiO_2 electrodes at open circuit have been shown[135] to compare well with the reduction rates calculated from the currents at the intersection of the photocurrent- and inverted dark current=voltage curves. The roles of light intensity, pH and platinization on the reduction rates of various relays have been discussed. The same authors [136] have observed that the consumption of holes produced upon 350-420nm irradiation of the TiO_2 sols or suspensions in polyvinyl alcohol/methylviologen system shows a significant dependence on the the bulk solution pH. An optimal quantity of OH^- ions was deemed necessary in order to allow for the specific adsorption of the polyvinyl alcohol onto the TiO_2 surface and favor its hole scavenging action.

In the presence of an adsorbed reactant (polyvinyl acohol or SCN^-) for positive holes produced in colloidal TiO_2 particles upon illumination, an excess of long-lived electrons remains on the particles and finally reacts with a substrate in the bulk solution. On the other hand, in the presence of an electron scavenger such as methylviologen or a deposited metal such as Pt, an

excess of long-lived holes remains which finallyreacts with an oxidizable compound. These processes were observed in the reduction of water to yield hydrogen, the reduction of $C(NO_2)_4$ and halothane, and the oxidation of Br^- and various organic compounds[137].

The photocatalytic oxidation of ethane over TiO_2 has been studied[138] at room temperature as a function of reactant partial pressure, UV light intensity, the amount of catalyst, and the residence time. On the basis of the experimental critical mass of the catalyst, an expression permitting the calculation of the critical mass of the TiO_2 catalyst for any type of photocatalytic reactor was derived]138]. Stepanenko and coworkers[139] have reported on the heterogeneous and homogeneous photooxidation of C_{2-5} hydrocarbons and 1-hexene in the gas and liquid phases using titanium-containing catalysts. The TiO_2-sensitized photooxidation of several benzenes has been examined in order to established the origin of the ring hydroxylating species[140]. In agreement with other studies, the major pathway for the formation of the hydroxyl group of phenols is pH-dependent. At low pH, the oxygen atom originates mostly from solvent water; whereas at higher pH, the hydroxyl group of phenols comes essentially from molecular oxygen.

The oxidation of CO with oxygen is catalysed by CoTPP (TPP = tetraphenylporphyrin) on TiO_2 at 194K. This catalyst exhibits unique features in terms of oxygen adsorption, the poisoning of adsorbed oxygen, and the insolubility of the complex in benzene[141]. Cyclohexene has been employed as an organic probe for the mechanism in the TiO_2-photocatalysed oxidation of bromide in acetonitrile[142]. The results suggest a mechanism in which the photoexcited semiconductor effects a one-electron oxidation of adsorbed bromide, yielding surface-bound bromine atoms. These could potentially abstract hydrogen from cyclohexene to initiate autooxidation, or could migrate along the semiconductor surface, producing Br_2, which migrates into solution where it is rapidly trapped in conventional electrophilic addition[143]. Rose and Nanjundiah[144] have measured the rate of photooxidation of CN^- by TiO_2

(anatase) as a function of TiO_2 particle size and platinization, and solution pH. The reaction rate constants increase with increasing TiO_2 particle surface area, with platinizing, and on lowering the pH from 14 to 11. Doped TiO_2(anatase) (with various elements) can photolyse the production of H_2SO_4 from sulfur in water into which oxygen was bubbled[145].

A pulse reactor and a continuous dilution flow reactor have been used to determine the activity of binary oxide catalysts in the dehydrogenation of ethylbenzene and ethylcyclohexane. The catalysts were composed of TiO_2 and other first period transition metal oxides. A mechanism is proposed, based on the correlation between the activity and the surface acid-base property[146]. TiO_2 has been incorporated into the catalyst system for the oxidative dehydrogenation of butane to maleic anhydride[147]. Ohtani et al. [148] find that extra-fine crystallites of brookite TiO_2 exhibits marked photocatalytic activity for the dehydrogenation of propan-2-ol in aqueous solution and silver metal deposition in Ag_2SO_4 solution.

Thiazine and oxazine dyes have been photoelectrochemically reduced in colloidal TiO_2 suspensions with bandgap excitation[149]; ^{57}Fe Moessbauer spectroscopy was employed to monitor the kinetics of the photoreduction of Fe^{3+} to Fe^{2+} via illuminated TiO_2 particles suspended in an $FeCl_3$ electrolyte [150]. For the latter study, a kinetic model was proposed, based on competition between the forward reduction of Fe^{3+} and the back oxidation of Fe^{2+} and controlled by semiconductor band/redox couple energetics. UV irradiation of TiO_2 anchored onto porous Vycor glass at 77K in the presence of N_2O or oxygen leads to the formation of an unstable nitrogen-containing radical (N_2O^- or $N_2O_2^-$) and the O_2^- anion radical, respectively[151]. The addition of oxygen onto the catalyst at 77K in the presence of the nitrogen-containing radical leads to the disappearance of the latter species and to the formation of O_2^-, which is suggestive that the electron transfer occurs easily between species adsorbed on the anchored TiO_2. The reactions were studied using ESR spectroscopy and isotopically labeled compounds.

Visible light hydrogen generation from water was observed from solutions containing a TiO_2 sol charged with a redox catalyst and containing 8-quinolinol metal complexes $M(QO)_n$ ($M = Pt^{2+}$, Pb^{2+}, Bi^{3+}, Ir^{3+}; $n = 2,3$) as sensitizers [152]. The reaction mechanism apparently involves electron transfer from the triplet excited state of the sensitizer into the conduction band of TiO_2. The most suitable sensitizers for water decomposition were $Ir(QO)_3$ and $Pt(QO)_2$. Bahnemann and coworkers[153] have established that the electrons and positive holes formed in TiO_2 suspensions upon exposure to UV light could be characterized by optical absorption. By direct detection of these surface states, a kinetic study of heterogeneous electron transfer reactions at the TiO_2/solution interface was performed. Also, by examination of the separation of the e^-/h^+ pair, it was possible to establish the chemical and physical principles of such reactions[153].

Several studies of the catalytic hydrogenation of CO and Co_2 and methanation of CO_2 as a function of the type of catalyst have been cited. Dao and Pruchnik[154, 155] have examined these reactions on catalysts prepared by the decomposition of palladium, nickel, cobalt and iron acetylacetonate (acac) complexes impregnated on γ-Al_2O_3 and γ-Al_2O_3. The additional presence of TiO_2 or MoO_3 in the Al_2O_3 enhances the activity of the palladium catalysts[154]. They also looked at the hydrogenation and methanation reactions over catalysts containing 0.7 wt% Rh, obtained by impregnation of $Rh(acac)_3$ on γ-Al_2O_3, TiO_2/γ-Al_2O_3, MoO_3/γ-Al_2O_3 and TiO_2-MoO_3/γ-Al_2O_3 [155]. The catalytic activity of Rh in the hydrogenation of CO and CO_2 was studied as a function of the electrical properties of the TiO_2 support[156]. This was accomplished by doping the TiO_2 with lower- and higher-valency cations. Doping with lower-valency ions (Mg^{2+}, Al^{3+}) hardly influences the electrical conductivity of TiO_2 or the specific activity of the Rh. An increase in the electrical conductivity of TiO_2 of 1-2 orders of magnitude was achieved by incorporating W^{6+} ions into the TiO_2. This favorable effect has been attributed[156] to the enhanced electron transfer from TiO_2 to Rh, which promotes the dissociation of

CO. Infrared spectroscopy and temperature-programmed techniques were utilized by He et al. [157] to examine and compare the interaction of $CO/CO_2/H_2$ with ZnO, TiO_2 and ZrO_2. The reactive characteristics of the oxides suggest that CO hydrogenation occurs via a formate-methoxide mechanism. It appears that TiO_2 does not hydrogenate CO or CO_2 into methanol[157].

The photolytic decomposition of phenol in oxygenated aqueous suspensions of lightly-reduced TiO_2(anatase) was investigated at the optimum pH 3.5 [158, 159]. The reaction followed first-order kinetics up to high conversions, for which the apparent rate constant depends on the initial phenol concentration, and an activation energy of 10 kJ/mol. The products at the initial stage of reaction were identified as hydroquinone, pyrocatechol, 1,2,4-benzenetriol, pyrogallol, and 2-hydroxy-1,4-benzoquinone. These intermediates undergo further photocatalytic oxidation, via acids and/or aldehydes, to CO_2 and H_2O. A reaction scheme involving OH radicals as real reactive species has been prepared[158]. Their formation occurs via holes and via H_2O_2 from oxygen.

Infrared spectroscopy and pulse reactor techniques were employed to monitor the isomerization of propylene oxide over TiO_2. A mechanism was inferred that involved an adsorbed substrate bound to the titanium atom through the oxygen atom[160].

Hydrated TiO_2 catalyses the esterification of phthalic anhydride by primary alcohols (Linevol 79) via formation of a homogeneous organotitanate catalyst species[161]. Proton nmr, infrared and Raman spectroscopies, as well as x-ray phase analysis and thermogravimetry were used to characterize the products of the reaction between $TiO_2 \cdot nH_2O$ and NaOH. The products contain three types of nonequivalent OH groups, bridging, terminal and hydrogen-bonded to water[162]. Dvernyakova et al. [163] have determined the composition of the thermolysis products of $TiO_2 \cdot nH_2O$, $CaCO_3 \cdot nH_2O$ and their 1:1 mixtures during heating at 423 - 1423K. Also investigated were the kinetics of the reaction of $TiO_2 \cdot nH_2O$ with $CaCO_3$, the dependence of the $CaTiO_3$ yield on the degree of dispersion of $TiO_2 \cdot nH_2O$, and the effect of the degree of dispersion of

$TiO_2 \cdot nH_2O$ on the crystal formation of $CaTiO_3$[163].

In the presence of TiO_2, CO_2 and SO_3 are produced *via* the photoinduced oxidation of *cis*-2-butene and SO_2, respectively[164]. A flow-type reactor was used to study the photocatalytic effects of TiO_2 on the photochemical reaction of *trans*-2-butene and *trans*-2-butene/NO_2/air systems. *Trans*-2-butene was rapidly oxidized to CO_2 by oxygen in the presence of TiO_2 under irradiation. Addition of NO_2 to the reaction system reduced the CO_2 yield, which indicates that NO_2 depresses the photocatalytic activity of TiO_2[165]. UV illumination of pre-oxodized or pre-reduced TiO_2 powder, which has been exposed to $N^{18}O$ in the dark at 295K, results in photoadsorption, photoexchange, and photodecomposition form N_2O and N_2. The addition of 2-butanol to $N^{18}O$ suppresses the isotopic exchange[166].

Malinowski and coworkers[167] have published a preliminary note on a study of reactions of organic substrates (methanol, acetone, acetic acid, ethylacetate, butyl acetate) on low-valent titanium heterogenized on SiO_2 or TiO_2 support materials. Theyalso compared these reactions with those in the in the presence of a homogeneous system. Comparative studies on the kinetics and mechanism of the chlorination of TiO_2(anatase) and V_2O_5 with CCl_4 were performed[168]. Approximate first-order kinetics were observed and an apparent activation energy of 118 ± 7 kJ/mol calculated for the chlorination of TiO_2. A dissociative adsorption of CCl_4 apparently precedes the reaction, and the transformation of CCl_4 to CO_2 was assumed to occur *via* the formation of an adsorbed $COCl_2$ intermediate[168].

Itaya *et al.* [169] have disucssed the electron transfer reactions in the open-spaced crystal of Prussian blue (PB) by photooxidation at n-TiO_2. The reduction of PB occurs at the TiO_2 electrode, though the corresponding oxidation is not possible in the dark.

4.7 OXIDES, $MTiO_x$

The molar enthalpies of reaction at 970K for the sodium and potassium

titanates in reactions 3 and 4 were determined by high-temperature

$$m\ Na_2TiO_3 + (n-m)\ TiO_2 \rightleftharpoons mNa_2O{\cdot}nTiO_2 \qquad (3)$$

$$m\ K_2TiO_3 + (n-m)\ TiO_2 \rightleftharpoons mK_2O{\cdot}nTiO_2 \qquad (4)$$

solution calorimetry; for which (m, n) = (1, 1), (4, 5), (1, 2), (1, 3) and (1, 6) in reaction 3, and (m, n) = (1, 1), (2, 3), (1, 2), (1, 4) and (1, 6) for reaction 4 [170]. The x-ray crystal structure of $Na_4Ti_5O_{12}$ reveals the compound to be monoclinic, space group C2/m, with corrugated layers of Ti_5O_{12} held together by sodium ions[171].

Balasubramanian[172] reported a new preparatory method for $SrTiO_3$; it involves the calcining (873K or 973K; 12 hrs) of crystals obtained by mixing solutions of EDTA complexes of strontium and titanium. The resulting $SrTiO_3$ product was characterized by crystal structure analysis, ESR spectroscopy and electrical conductivity measurements.

A photoelectrochemical system composed of $SrTiO_3$ single-crystal electrodes as electron acceptors and two adsorbed cyanine dyes (2,2'-diethylthiacarbocyanine and 2,2'-diethyloxadicarbocyanine) in their excited states (electron donors) was examined in terms of the energetic threshhold for dye-sensitized photocurrent at the electrode[173]. The heats of adsorption (6 - 10 kcal/mol) show the dye molecules are weakly adsorbed by the electrode, while fluorescence spectra of the dyes revealed the influence of pH on the photophysics of the dyes. The oxidation potentials of the dyes were evaluated by cyclic voltammetry; the $SrTiO_3$ electrodes show a pH dependent flatband potential. The photocurrent is also pH-dependent[173]. The photoelectrochemical properties of Nb_2O_5, Sb_2O_3 and V_2O_5 doped

on $SrTiO_3$ ceramic electrodes were reported by Yoon and Kim[174]. Irradiation of an electrochemical cell consisting of a semiconductor (TiO_2, $SrTiO_3$) anode, a metal cathode, and an aqueous electrolyte solution with ionizing radiation stimulated the electrochemical decomposition of water. The ionizing radiation was in the form of accelerated electrons with energy 4 MeV, x-rays of 70 keV, γ-rays, and neutrons from a nuclear reactor[175].

The preparation of $BaTiO_3$ *via* thermal decomposition of $BaTiO(C_2O_4)_2 \cdot 4H_2O$ has been simultaneously examined by emanation thermal analysis, thermogravimetry, DTA and evolved-gas analysis [176]. Nabivanets and Omel'chenko[177] have looked at the optimum conditions (pH and component concentrations) for the production of $BaTiO_3$ *via* coprecipitation by examining the solubility in the $BaCO_3$ -- $Ti(OH)_4$ -- $NaHCO_3$ -- H_2O system. The photoelectrochemical behavior of donor-doped $BaTiO_3$ ceramic anodes has been compared with that of hydrogen-reduced $BaTiO_3$ and hydrogen-reduced $SrTiO_3$ [178]. Donor-doped $BaTiO_3$ has a response to visible light without mechanical polishing and seems unaffected by chemical etched. Hydrogen-reduced $BaTiO_3$ also has photoresponse in the visible; however, it is modulated upon mechanical polishing.

The catalytic decomposition of N_2O was studied as a function of 'x' over $Sn_{1-x}V_xO_2$ and $Ti_{1-x}V_xO_2$ ($0 \leq x \leq 0.2$) solid solution. The catalytic activity decreases as a function of the V content up to $x = 0.03$, then increases as x increases. The surface activity correlates with varying the charge transfer effects in the catalyst as x increases. The variations of activity appear to be related to the developing electronic state of a V sublattice[179]. Thermal decomposition of $Ti_{1-x}Cr_xO_{2-x}(OH)_x$, with the In OOH-type structure, results in the formation of the mixed rutile-type oxides $Ti_{n-2}Cr_2O_{2n-1}$[180].

Single phases of $Fe_{1-a}Ti_aO_y$ (phase I, rhombohedral, y = 1.5, a = 0.5, 0.42, 0.35, 0.25; phase P, orthorhombic, y = 1.67, a = 0.67, 0.6, 0.5, 0.33; phase S, spinel, y = 1.33, a = 0.27, 0.2) have been prepared by solid-state reactions of Fe_2O_3, TiO_2(rutile) and iron carbonyl at 1323 - 1573K[181]. The electronic structures of TiO_6^{8-}, TiO_6^{9-} and TiO_6Fe_4 clusters, which simulate TiO_2, Ti_2O_3 and $FeTiO_3$(ilmenite) crystals, respectively, were determined by the SCF-X_α scattered-wave method. The dependence of the electronic structure spin density distribution on the number of unpaired electrons in the Fe atoms has been reported for the TiO_6Fe_4 cluster. The spin densities of the Ti and Fe atoms were shown [182] to interact via O atoms (i.e., indirect exchange interaction).

Zunic and coworkers[183] have determined the x-ray crystal structure of a modification of $ThTi_2O_6$, obtained from the melt at 1373K. The crystal is monoclinic, with near-hexagonal close-packing of the O atoms, and Th and Ti atoms occupy octahedral sites. The coordination about Ti is a distorted octahedron; about Th, it is a distorted square antiprism. The Ti coordination polyhedra form layers parallel to the (100) face and are connected by zigzag chains of the Th coordination polyhedra which run in the [001] direction[183].

4.8 OXIDES, M/TiO_2

In the dynamic V_2O_5/TiO_2(anatase) system, the state of vanadium depends on the loading of V_2O_5 and the calcination temperature. Vanadium is present as a surface species coordinated to the TiO_2(anatase) surface at low contents of V_2O_5 on TiO_2. At intermediate V_2O_5 contents on TiO_2, V is also present as V_2O_5 crystallites. At high calcination temperatures, the ratio of

surface vanadium and V_2O_5 crystallites is affected, with consequential formation of a $V_xTi_{1-x}O_2$ solid solution[184]. Busca et al. [185] have characterized the surface of a low-content vanadium catalyst, prepared by grafting a high-surface-area TiO_2 support. The methodologies employed include diffusion reflectance, ESR and Fourier-transform infrared spectroscopies. The grafting reaction of vanadium takes place on all surface OH groups of TiO_2, leaving Ti^{4+} exposed. The vanadium sites are isolated on the surface and have labile oxidative and coordinative states[185]. It has been shown[186] that oxygen adsorption isotherms at 273 - 723K and 0.05 - 2 torr obey the Langmuir model for the adsorption of molecular oxygen on the V_2O_5/TiO_2 systems. The two maxima observed at 523 and 673K in the 0.55 torr adsorption isobars have been ascribed to O^{2-} chemisorption and to its diffusion to the microcrystal interior, respectively. Raman spectroscopy and XPS were utilized to characterize the small V_2O_5 crystallites supported on TiO_2(anatase) in situ under oxidizing and reducing conditions at elevated temperatures. At such temperatures, the V_2O_5 crystallites are readily reduced by hydrogen to V_2O_3, and reoxidized to V_2O_5 crystallites in flowing air[187]. Emf measurements have also been carried out to determine the formation thermodynamic (partial) functions of V_2O_5 solid solutions with TiO_2 at several temperature intervals[188].

Rusiecka[189] has characterized the active phase of the V_2O_5/TiO_2 catalysts by ESR spectroscopy. Various amounts of V_2O_5 ($\leq$20 mol%) were deposited on TiO_2(anatase, rutile), and ESR spectra of the samples recorded initially, after catalytic oxidation of o-xylene, and after reoxidation in air. The amount of reduction taking place on the catalyst during reaction was determined by the strength of the V^{4+} signal[189]. The observed

low selectivity for phthalic anhydride during o-xylene oxidation was explained[190] by the formation of needle-shaped crystallites of V_6O_{13} at low vanadium concentrations on V_2O_5/TiO_2(anatase) coated catalysts. ESCA, x-ray diffraction, SEM, and infrared and ESR spectroscopies were used to characterize vanadium oxide/ titanium oxide catalysts in relation to activity and selectivity for oxidation and ammoxidation of alkylpyridines[191].

Electron microscopy and electron diffraction studies of V_2O_3-doped TiO_2 reveal the presence of two different types of planar defects[192]. At dopant concentrations <3%, isolated (101) and (132) faults appear, while at V_2O_3 concentrations >5%, an ordering of the defects is observed. At [V_2O_3] up tp 13%, a new family (M_nO_{2n-1}, M = V+Ti) of ordered phases forms[192].

Several groups[193 - 197] have studied oxidation reactions catalysed by V_2O_5/TiO_2. German and coworkers[193] investigated these catalysts calcined at 973 - 1273K in the ammoxidation of β-picoline and 5-ethyl-2-methylpyridine. The optimal calcination temperature was found to be 1073K. The kinetic study of low-temperature oxidation of toluene and its derivatives over V_2O_5 and V_2O_5/TiO_2 in a differential flow reactor reveals that complete oxidation follows the mechanism of conjugate reoxidation of the catalyst surface[194]. Rate constants for the ammoxidation of MeC_6H_4R (R = H, 3-Me, 3-CN, 3-NO_2, 3-Cl, 2-OH, 2-NH_2, 2-Br), pseudocumene, mesitylene, MeC_6H_4R' [R' = 3,5-$(CMe_3)_2$, 2,6-Cl_2], 5-tert-butyl-m-xylene, durene and 2,3,5,6-tetrachloro-4-tert-butyltoluene were established at 653K. It appears that (a) o-cresol is the most reactive, (b) 2,3,5,6-tetrachloro-4-tert-butyltoluene is the least reactive, (c) reactivity decreases in the presence of benzene, and (d) the reactivity increases with basicity in the order toluene, pseudocumene, and mesitylene[195].

Skrzypek et al.[196] suggested that in the catalytic air oxidation of o-xylene over V_2O_5/TiO_2, the limiting step can be described by the Langmuir-Hinshelwood kinetic model, wherein a surface reaction between o-xylene and oxygen occurs, chemisorbed on separate active sites. In another study, the interaction of V_2O_5 with TiO_2 (anatase) in the o-xylene oxidation reaction has been examined [197].

Measurable catalytic activity in the gas-phase water decomposition reaction under illumination with bandgap light has been observed in the presence of a Ta-doped TiO_2 catalyst, previously prereduced and coated with NaOH[198]. Rate enhancement occurs upon addition of RuO_2.

$[Ti/Cr_2O_3 + TiO_2]$ composite electrodes, prepared by a ceramic method, have been used in the heterogeneous anodic oxidation of aliphatic alcohols and ethers in 1M H_2SO_4[199]. A new catalyst for the oxidation of butene to maleic anhydride has been reported. The highest selectivity is observed for the catalyst composed of U--Mo--O supported on TiO_2, with U/Mo = 1/10 and Mo/Ti = 1/8. X-ray diffraction, and infrared and UV-visible spectroscopies revealed the existence of UO_2MoO_4, MoO_3 and TiO_2 phases[200]. Liu and coworkers[201] studied catalyst structure and reaction selectivity for the photooxidation of methanol catalysed by supported MoO_3/TiO_2. Although the photo-efficiency of the MoO_3/TiO_2 catalyst is about one-fifth that of pure TiO_2, the enhanced selectivity in suppressing secondary oxidation reactions is significant.

Sun and Ding[202] have prepared a catalyst containing 3% Fe_2O_3 supported on TiO_2 by impregnating TiO_2 with a solution of $Fe(NO_3)_3$, and subsequently drying it at 373K and calcining at 823K for 5 hr. The catalyst was then characterized at various

steps in the water-gas shift reaction. Other supports (MgO, γ-Al_2O_3) were also employed and comparisons made[202]. Moessbauer spectroscopy has been used to study the interaction of the coordinatively unsaturated sites of TiO_2 supporting Fe or Fe-Ir. It would appear that the coordinatively unsaturated sites of TiO_2 serve as a template for Fe^{2+} as well as for the Fe-Ir cluster[203].

X-ray, Moessbauer and ESR emthods were used to elucidate the structure of TiO_2-Fe_2O_3 polycrystalline solids containing 0 - 10% Fe. The catalysts were prepared by coprecipitation and by impregnation, and treated in air at 773 - 1273K. The method of preparation is discussed in relation to photocatalysis in the photoreduction of dinitrogen to ammonia[204]. The nature of the surface species present on 10% Fe/TiO_2 in the low-temperature reduced state (558K) has been investigated[205] after short reaction times in 10% CO/H_2 at 558K and 1 atm pressure. The results show that the surface is covered with approx. 46 µmol/g of CH and large quantities of surface carbidic carbon during reaction. The first growth stages of ultrathin films of iron and platinum deposited on the (001) face of TiO_2 have been characterized[206] by Auger electron spectrscopy (AES), secondary electron emission and work function changes. Thorp and Eggleston [207] have monitored the changes in the amplitude of the Fe^{3+} feature in the ESR spectra of a series of pigment-like Fe-doped TiO_2 powders during and subsequent to optical irradiation. Doping levels were in the range 30 - 670 ppm Fe. In contrast to what has been reported for Fe-doped single-crystal TiO_2, the Fe^{3+} concentration in these powders is affected only by light of wavelength >700nm. The results are discussed in terms of the deep impurity level system proposed in 1979 by Mizushima and coworkers [207].

The morphology and microstructure of thin films (15 - 20nm) of composition $xRuO_2$--$(1-x)TiO_2$ have been determined by electron diffraction and electron microscopy. These films represent the microheterogeneous system formed of finely dispersed rutile-type phases of TiO_2 and RuO_2[208]. The electrocatalytic redox mechanism of the ruthenium oxide/titanium oxide system in relation to its use in chlorine manufacture *via* electrolysis was investigated by x-ray excited photoelectron spectroscopy (XPS) [209]. The growth of the pyrolytic RuO_2/TiO_2 interface was observed step-by-step after 1, 3, 5, 10 and 25 coatings. Kishi [210] has reviewed the laboratory-scale preparation, characterization and electrochemistry of RuO_2/TiO_2 type dimensionally stable anodes. TiO_2 containing a few percent ruthenium was investigated by ESR and x-ray diffraction. Prolonged treatment in hydrogen at <623K or the addition of Nb(V) to the rutile structure gives paramagnetic Ru(III) in solid solution. On increasing the temperature of the hydrogen treatment, reduction to Ru(II) in solid solution occurs, followed by reduction to Ru(O) as a segregated phase[211]. Bartelt[212] has discussed the properties and advantages of RuO_2/TiO_2 anodes, as well as improvements of the anodes by insertion of an intermediate layer of electrically well conducting oxides, active layer modification, or changes in the anode electrochemical parameters. In fact, the degradation mechanism of electrodeposited β-PbO_2 on a RuO_2/TiO_2-loaded titanium substrate has been studied[213]. An XPS study of the RuO_2/TiO_2 surface electron configuration has been reported, as well as the effects of surface oxidation and reduction processes[214]. Blazey and coworkers[215] have shown, by paramagnetic resonance studies, the presence of both $Ru^{5+}(4\underline{d}^3)$ and $Ru^{3+}(4\underline{d}^5)$ in oxygen octahedral coordination of TiO_2 single

crystals doped with ruthenium.

A radiochemical study reports on the dissolution selectivity of the components of RuO_2/TiO_2 anodes in chloride solution carried out as a function of pH at an anodic current density of 0.2 A/cm^2 and 363K. The selectivity is explained in terms of the presence of the components in the coating composition, not only in the combined oxide form, but also as individual phases[216]. The same authors[217] also investigated this selectivity as a function of the phase composition of the coating and the corrosion resistance of the coating as a function of it's composition. RuO_2/TiO_2 anodes can be prepared by applying solutions of ruthenium chloride hydroxide and $TiCl_4$, drying at 423K, and decomposing at 723K. The anodes were analysed by PIXE spectroscopy with a germanium detector, and the relative loss of ruthenium during thermal decomposition was determined to be ≈21%[218].

The corrosion resistance of RuO_2/TiO_2 anodes has been determined during electrolysis of seawater[219] and chlorate electrolysis[220]. The effect of low chloride content and the changing temperature of seawater in the electrolysis precess on anode corrosion resistance has been investigated[219]. The chlorate electrolysis, a neutron activation method was used to determine the effect of the composition of the $NaCl--NaClO_3$ electrolyte[220].

Various groups have examined the oxygen evolution from chloride solutions at RuO_2/TiO_2 anodes. Quam and Yin[221] have examined the effect of pH on the kinetics of oxygen evolution. Two methods have been described[222] for determining the rate of oxygen evolution: one is based on the use of the effect of equivalent acidification of a solution as a result of oxygen evolution; the other is based on compensation of the equilirium value during contact of the anode with a chlorinated sol. Bune

et al.[223] have described a method which allows the determination of the effect of anode composition and solution composition on the kinetics of the secondary reaction of oxygen evolution under chlorine electrolysis conditions. Both Bune[224] and Kokoulina [225] and their coworkers have investigated the influence of anions on the kinetics of the oxygen evolution reaction. Specifically, polarization curves were obtained in acid and alkaline perchlorate, sulfate, and phosphate solutions and in acid chloride solutions. In the presence of the more strongly adsorbed anions, some increase in oxygen overvoltage was observed [225]. Polarization measurements as well as gas chromatographic analyses of the composition of gaseous products of the elecrolysis were utilized to determine the effect of foreign anions (sulfate, phosphate, perchlorate) on the reaction kinetics[224].

An analysis of the mechanism of chlorine reaction at RuO_2/TiO_2 anodes has appeared in the Russian literature[226]. The hydrogenation of CO catalysed at ≈500K by (a) 17% Ru/TiO_2, (b) 2.6% Ru/SiO_2, (c) 1.5 Ru/13x-zeolite and (d) 5% Ru/MgO yields methane and 1-alkenes as primary products. Specific activity of the catalysts varies in the order (a) >> (c) > (b) > (d); whereas selectivity for methane formation varies as (b) > (c) > (a) > (d). The single most important factor in determining the total product distribution is the availability of adsorbed hydrogen, which varies in the order (b) > (c) > (a) > (d)[227].

Titanium dioxide-supported cobalt catalysts, prepared by alkoxide and impregnation emthods, have been examined by EXAFS in order to identify the local structures which contribute to the superior properties of catalysts prepared by the alkoxide method [228].

Sun and coworkers[229] have reviewed work on strong metal-

support interaction (SMSI) using rhodium or platinum deposited on TiO_2 thin films. Results from thernal desorption spectroscopic, AES and static SIMS experiments are discussed. A method has been reported[230] for the preparation of new catalysts containing $ORhC_3H_5$ (C_3H_5 = allyl), ORhH and $[Rh]_n$ moieties. They were prepared *via* reaction of $Rh(\ ^3\text{-}C_3H_5)_3$ with surface OH groups of TiO_2, followed by chemical treatments with hydrogen. The catalysts reportedly show higher activities for C_2H_6 hydrogenolysis and C_2H_4 hydrogenation than a conventional impregnation rhodium catalyst[230].

Shpiro *et al.*[231, 232] have explored the nature of the strong interaction between metal(Rh) and support (TiO_2) using x-ray photoelectron and secondary-ion mass spectra. The results are indicative of a local interaction between Rh and reduced Ti cations as a consequence of high-temperature reduction of Rh/TiO_2 [231]. Surface-sensitive electron spectroscopies, CO chemisorption measurements, and Auger sputter profiling were employed to study the SMSI in Rh/TiO_2 model catalysts. Further, the oxidation dynamics of reduced TiO_2 surfaces as a function of annealing temperature were examined. The high temperature reduction of $Rh/TiO_2(110)$ catalysts to an SMSI state is reportedly accompanied by the formation of a suboxide of Ti on the Rh particles, thereby blocking CO chemisorption sites[233]. Samples of Rh/TiO_2 and $Rh/SrTiO_3$ catalysts, subjected to thermal treatments under hydrogen and *in vacuo*, have been examined by nmr, ESR and quantitative adsorption techniques to ascertain the dependence of SMSI effects on hydrogen strongly adsorbed at high temperatures [234]. The loss of H_2 chemisorption capacity upon high-temperature reduction occurs only in Rh/TiO_2, and is accompanied by extensive incorporation of hydrogen in the support in the form of

hydride-type species.

An nmr study of hydrogen adsorption on Cl_3Rh/TiO_2 catalysts reveals the presence of two types of adsorbed hydrogen on the metal and the modification of the metal-hydrogen interaction with the extent of the adsorption[235]. The hydrogen reduction of Rh/TiO_2-V_2O_5 and Rh/V_2O_5 catalysts at $\geq$298K was investigated by Miller and coworkers[236]. The results are consistent with the formation of H^+ species during metal reduction and spillover hydrogen atoms during support reduction.

The support interaction between rhodium and TiO_2 supports has been investigated by several groups for the catalysed carbon monoxide hydrogenation reaction. Catalysts composed of 1-2 wt% Rh supported on TiO_2 were employed for hydrogenation of CO to C_{1-6} hydrocarbons, methanol and ethanol. At 0.13-1.20% C conversion, Richards and Newman[237] find no specific selectivity to any single product, though temperature-programmed reduction was interpreted in terms of the presence of both bulk Rh (weak support interaction) and dispersed Rh (strong support interaction) species. Catalytic activity is significantly influenced by reduction conditions, to give maximum activity per weight for reduction at 673K for 2 hr[238]. Tamaru and coworkers[239, 240] have examined highly loaded (25 and 60 wt%) Rh/TiO_2 for CO hydrogenation, as well as the effects produced on varying the pretreatment conditions, the supports and the metal precursors [241]. For the 25 wt% Rh/TiO_2 catalyst subjected to reduction at 573 and 723K, the Rh/TiO_2 ratio lies in the strong metal-support interaction range (SMSI) after reduction. The catalytic activity is significantly lower in the SMSI state than after reduction at low temperatures[239]. Moreover, the studies support the view that SMSI is due to migration of TiO_x ($1 < x < 2$) on the metal

surface[240]. Chuang and coworkers[242-244] have reported on the effects of alkali metal addition on the hydrogenation of CO over Rh/TiO_2. The rate of CO conversion, as well as the hydrogenation activity of the catalysts, decreases in the order: unprotonated > Li > K > Cs [242, 244]. The ability of the alkali species to promote the selectivity for oxygenated compounds apparently increases in the order: unprotonated < Li < K ≈ Cs [243]. The activities and selectivities of Rh/TiO_2 and alkali-promoted Rh/TiO_2 appear to be correlated with their catalytic abilities for hydrogenation, CO dissociation and CO insertion.

The rate of hydrogenation of several unsaturated compounds mediated by $Rh-Ru/TiO_2$ catalysts decreases in the order: 1-hexene > cyclohexene > o-nitrophenoxide > $MeC{\equiv}CCH(OH)Me$ > Me_2CO [245].

Rh/TiO_2 is known to be a very active catalyst for the methanation of carbon monoxide with water. The presence of platinum further enhances the catalytic activity[246]. In a study of this reaction over Rh/ZrO_2, Rh/Al_2O_3, Rh/TiO_2, Rh/SiO_2, and Rh/MgO catalysts, high activity was achieved for Rh/ZrO_2 and Rh/TiO_2 at 573K. Also, the CO dissociation ability of the catalyst appears to be an important factor in obtaining high activity[247]. Methane formation appears to occur through the water-gas shift reaction, followed by hydrogenation of carbonaceous species formed *via* CO (or CO_2) dissociation.

Infrared spectrscopy was instrumental in the examination of carbon monoxide and oxygen over supported rhodium films. The reactivity was investigated for various CO/Rh/M (M = Al_2O_3, SiO_2, TiO_2) ratios[248].

Yamaguti and Sato[249] examined the simultaneous production of hydrogen and oxygen upon photolysis of water vapor on NaOH-coated Rh/TiO_2 and Pd/TiO_2 catalysts. The rate of water

photolysis seems strongly dependent on the amount of NaOH loaded on the catalyst, and on the water vapor pressure. The maximized photolysis rate on the Rh/TiO_2 catalyst obtains for 15 wt% NaOH coating and 2 toor of water pressure. The relationships between photolysis rate and light intensity, wavelength and thernal back-reaction rate were also explored[249].

Catalysts of nickel supported on TiO_2, BeO. MgO, ZnO, Al_2O_3, Cr_2O_3, SiO_2, ZrO_2, ThO_2 and UO_2 have been prepared by coprecipitation with different precipitants and by impregnation of the basic nickel carbonate with a salt of the support[250]. The least efficient support for nickel dispersion is TiO_2, while the most efficient supports appear to be SiO_2 and Al_2O_3. The following observations were also made: i) each support increases the specific catalytic activity value of nickel with respect to unsupported nickel; ii) the specific catalytic activity increases up to a limiting value as the support content increases; iii) the most efficient supports in the hydrogen-water deuterium exchange reaction are TiO_2 and Zr_2O_2; and iv) the influence of the support on the specific catalytic activity is due to the participation of the support surface in the activation of the water molecule[250]. Controlled-atmosphere electron microscopy and gravimetric measurements were performed to determine the effects of depositing powdered TiO_2 on nickel surfaces with respect to the formation of filamentous carbon from acetylene and ethane[251]. Filamentous carbon formation is suppressed initially on those portions of the nickel surface containing TiO_2 when samples are directly heated in a hydrocarbon environment to 1000K. However, effective passivation of the nickel surface is achieved at all temperatures *via* pretreatment of the TiO_2/Ni samples in hydrogen at approx. 770K. The results obtained indicate that reduced TiO_2 species

migrate over metal surfaces under reducing conditions and collect into TiO_2 particles under oxidizing conditions. Thus, the idea that reduced TiO_2 species on metal surfaces may be the origin of SMSI for titania-supported metal particles is confirmed[251]. Malinkowski et al.[250] have examined supported titanium and Ni-Ti catalysts and non-supported Ni-Ti catalysts in the Fischer-Tropsch reaction at 523-573K. The supports included TiO_2, SiO_2, Al_2O_3 and HZSM-5 zeolite. The presence of titanium increases the yield of higher hydrocarbons in the reaction[252].

The Russian literature cites an electron microscopic study of TiO_2/Pd and ZnO/Pd thin film systems modeling the surface layer of a catalyst[253].

The kinetics and mechanism of platinum deposition by photoelectrolysis in illuminated suspensions of TiO_2 have been established. It has been proposed[254] that the TiO_2 particles are subject to strong internal electric fields which lead to efficient hole-electron-pair separation, yet these particles contain a large number of traps that cause recombination. Sato [255] has prepared Pt/TiO_2(anatase) catalysts by the photoelectrochemical deposition of Pt from a H_2PtCl_6 solution, and characterized their properties for CO and H_2 adsorption by infrared spectroscopy and volumetric analyses. Apparently, i) dispersion of Pt depends on the commercial source of TiO_2, ii) good Pt dispersion is achieved by photodeposition of Pt followed by photoreduction employing a sacrificial reducing agent, and iii) Pt dispersion is lowered by photoelectroplating the Pt in the presence of the reducing agent. Also, photoimpregnation of H_2PtCl_6 followed by calcination in air and reduction in hydrogen yields well-dispersed Pt/TiO_2[255]. Moessbauer spectroscopic methods were utilized to elucidate the sorption of platinum(II)

chloro complexes from $K_2[PtCl_4]$ solutions on $TiO_2 \cdot nH_2O$ modified by tin(II) compounds[256]. The complex sorption mechanism is thought to involve ion exchange, and complexing and oxidation-reduction reactions.

Titanium dioxide gels containing platinum and ruthenium have been prepared by calcining hydrogels made by the hydrolysis of a mixture composed of titanium(IV) oxide hydrosol, H_2PtCl_6, $RuCl_3 \cdot xH_2O$, and various alkali hydroxides[257]. In the presence of such gels, evolution of hydrogen occurs upon radiation (500W high-pressure mercury lamp) of a methanol-water mixture. The rate of hydrogen evolution depends on the amount and type of alkali hydroxide used in the gel preparation. X-ray diffraction studies show that the fractions of microcrystalline anatase- and rutile-type modifications formed in the TiO_2 gels varies with the alkali hydroxides employed[257].

Recent examinations of SMSI in Pt/TiO_2 catalysis attribute the inhibition of chemisorption and catalysis to the presence of a reduced titanium oxide, TiO_x, on the surface of Pt crystallites. Spencer's[258] equilibrium calculations show that titanium, dissolved in platinum <u>in vacuo</u>, is unlikely to segregate to the crystallite surface, though any traces of H_2O (present under normal reducing conditions) would be sufficient to give adsorbed oxygen on surface titanium atoms thereby greatly enhancing surface segregation. The calculated rates of diffusion, either Ti in Pt metal or adsorbed species on the Pt surface, are too slow at low temperatures for significant SMSI to occur, even though adsorbed TiO_x is stable under both high- and low-temperature reducing conditions[259]. The failure of Pt/TiO_2 catalysts to show SMSI effects after low-temperature reduction has bewen attributed[260] to kinetic, rather than equilibrium, limitations. Two possible

ways of forming the TiO_x layer are proposed with (i) being more important: (i) formation of TiO_x at the Pt/TiO_2 interface, followed by transport across the Pt surface; (ii) reduction of TiO_2 to yield a Pt/Ti alloy, followed by diffusion, surface segregation and oxidation[260].

Small-angle x-ray scattering measurements have been carried out on TiO_2 supports and Pt/TiO_2 catalysts that were reduced at low and high temperatures[261].

Chemisorption of H_2, CO and O_2 on 2 wt% Pt/TiO_2 was examined to establish a satisfactory method for measuring the Pt dispersion on TiO_2[262]. High-temperature reduction of Pt/TiO_2 results in a sharp decrease in H_2 and CO chemisorption capacities and catalytic activity. Oxidation-reduction treatments restore the usual catalyst properties. The magnitude of H_2 uptake suppression (and thus in SMSI formation) increases at higher TiO_2/Group VIII metal ratios, as does higher reduction temperature and extended reduction times at a given elevated temperature[263].
Differential scanning calorimetry has been used to determine isothermal, integral heats of adsorption of H_2 and CO on Pt/M (M = TiO_2, SiO_2, η-Al_2O_3, and SiO_2-Al_2O_3). A comparison of the results for the various supports suggests that the adsorption capacity for CO and H_2 can be decreased by an alteration in the chemical nature of surface Pt atoms, as well as by the physically blocking the Pt surface by migrating TiO_x species[264]. Vannice and coworkers[265] have reported on Auger electron spectroscopic (AES) and electron-stimulated desorption (ESD) experiments on titanium dioxide single-crystal and powder surfaces in the presence and absence of platinum.
Evidence of the structural interaction between Pt and TiO_2 can be obtained from TEM studies on the morphology of the Pt/TiO_2

surface. On heating the Pt/TiO_2 catalyst at 873 - 973K in a hydrogen atmosphere, the highly dispersed Pt is transformed into polygonal particles, possessing an epitaxial multiplane structure. The appearance of η-TiO_2 defect in the vicinity of the Pt and TiO_2 contacting point is likely the direct cause of epitaxial growth of Pt microparticles. Chen et al.[266] suggested the presence of a metal-semiconductor interaction for the Pt/TiO_2 system as an explanation for the observed morphology.

The electrochemical behavior of platinized TiO_2 electrodes has been examined in order to understand the role of the Pt layer on the TiO_2 electrode in photoelectrochemical and photocatalytic reactions. Platinization of single-crystal electrodes causes an increase in the rate of hydrogen evolution reactions, but does not affect the kinetics of oxygen evolution. However, both hydrogen and oxygen evolution reactions are accelerated upon platinization of polycrystalline TiO_2 electrodes[267]. The results show that the electronic equilibrium between Pt and the TiO_2 single crystal is established only when TiO_2 is biased relatively negative such that bands bend down towards the surface (or up only a small amount), but equilibrium between Pt and polycrystalline TiO_2 is always attained. So, for single-crystal TiO_2, it should be difficult to transfer electrons to Pt when TiO_2 is anodically polarized due to a relatively thick tunnelling barrier. By contrast, polycrystalline TiO_2 contains many impurity levels, grain boundaries, etc., such that electrons can be transferred from TiO_2 bulk to Pt via these levels. A drastic decrease in photocurrent at a TiO_2 electrode modified with Pt has been observed, in contrast to a 70% increase in photocurrent for a TiO_2 electrode modified with photodeposited gold[268]. The photocurrent inhibition is the result of the inability of

photodeposited or electrodeposited platinum to reach a saturation level on TiO_2, but rather continue to form deposits at the electrode surface.

TiO_2 overlayers on polycrystalline platinum were characterized by XPS. Vacuum annealing of the TiO_2 thin films has two significant effects: (a) most of the Ti^{4+} is reduced to Ti^{3+}; and (b) an equilibrium coverage of the reduced species is attained for initial coverages of $TiO_2 \geq 0.9$ monolayer. Depth profiles of annealed and non-annealed surfaces indicate that the reduced TiO_2 species diffuses into the Pt[269]. Ko and Gorte[270] have examined the interactions between oxide support materials (TiO_2, Al_2O_3, SiO_2, Nb_2O_5) and clean platinum foil. For all of the oxides, temperature-programmed desorption shows no change in the adsorption behavior of H_2 or CO. For TiO_2, AES results are indicative of the presence of segregated layers evenly covering Pt; complete suppression of H_2 and CO adsorption occurs at an oxygen coverage of 1×10^{15} cm^{-2}[270].

Ammonia is photocatalytically formed from an aqueous solution of azide ion using illuminated Pt/TiO_2 semiconductor powder. Reaction products include N_2, NH_3 and small amounts of N_2O and NO_3^-[271]. Photolysis ($\lambda_{ex} > 300nm$) of Pt/TiO_2 suspended in an argon-purged acetonitrile solution of aliphatic or aromatic primary amines gave Schiff bases, H_2 and NH_3 at room temperature [272].

In the hydrogenation of acetone to isopropanol at 330K over 0.5% Pt/TiO_2, conversions of 75% with selectivities $\geq$98% are routinely achieved[273]. The results reveal that conversions decrease linearly with the reciprocal of the flow rate when the reaction is carried out in a continuous-flow microcatalytic reactor at a flow rate of 40 ml/min. Thus, reaction on the

catalyst surface was rate limiting. Kunimori and coworkers[274] observed a significant decrease in the catalytic activity for the CO + H_2 reaction over Pt/TiO_2 after high-temperature reduction at 773K. However, the catalytic activity almost recovered during the reaction, due to the reverse effect of oxygen atoms (or water molecules) formed. It has also been observed, by Damiani and Butt [275] that high-dispersion Pt/TiO_2 catalysts in the normal state are slightly more susceptible to CO poisoning in the hydrogenolysis of methylcyclopropane than are comparable Pt/SiO_2 or Pt/Al_2O_3 catalysts.

Inasmuch as it is known that the surface properties of Pt/TiO_2 are altered upon high-temperature hydrogen treatment, Lin et al.[276] have examined the influence of the change in surface properties of Pt/TiO_2 on the electron transfer process across the solid-liquid interface, as studied by a dynamic potential sweep method for the liquid-phase photoreaction of carbon monoxide and water. Results show the following as a result of high-temperature hydrogen treatment: (i) a strong metal-semiconductor interaction between Pt and TiO_2 occurs; (ii) electronic contact between Pt and TiO_2 gradually changes from a Schottky to ohmic nature; (iii) the production of additional surface states; and (iv) a decreased energy barrier at the Pt/TiO_2 interface. It was proposed that the change in the surface properties of Pt/TiO_2 could bring about the direct charge transfer between CO and the Pt/TiO_2 photoelectrode [276]. Kolchanova and Mikheeva[277] reported the reversible deactivation of sodium-promoted Pt/TiO_2 catalysts for the oxidation of CO. The deactivation is reportedly due to increasing the strength of the Pt—CO bond, attributed to the variations in the chemical composition and structure of the CO-cotaining platinum compounds.

Pt/TiO_2 particles have been prepared from dispersions of clean colloidal Pt and TiO_2 particles. It was shown[278] that the binding of Pt to TiO_2 is primarily electrostatic in origin, and is only slowly reversed by charge reversal on the TiO_2 particles. Additionally, maximum coverage of Pt and TiO_2 is attained at pH 3 and corresponds to ≈20% of geometric close-packing due to lateral repulsions between bound Pt partilces. The adsorption of EDTA suppresses the binding of the Pt to TiO_2, and causes coagulation of Pt/TiO_2 particles. The Pt/TiO_2 catalyses the oxidation of the donors EDTA and oxalate when irradiated with light of energy greater than the bandgap of TiO_2. Rates of hydrogen production obtained as a function of irradiation time, ionic strength of the solution, addition of polyvinyl alcohol, Pt concentration, and TiO_2 concentration have been determined[279]. Loy and Wolf[280] developed a flow-reaction system to study the steady-state kinetics of hydrogen evolution by photodissociation of water in the presence of $Ru(bpy)_3^{2+}$ (bpy = 2,2'-bipyridine), MV^{2+} (methyl viologen), EDTA, and heterogeneous Pt/TiO_2 supported catalyst. Over a large range of reactant and catalyst concentrations, the reaction is zero-order, and does not exhibit Arrhenius-type behavior[280]. Water is reduced under UV illumination in a system consisting of $Rh(bpy)_3^{3+}$/dextrose. The reaction is enhanced by TiO_2-supported Pt[281]. A photocatalyst for decomposition of water has been prepared by photoplatinizing TiO_2(anatase) powder and dispersing it into an aqueous polymer solution. The polymer was prepared <u>via</u> reaction of $[Ru(bpy)_2\{4-(5-bromopentyl)-4'-methyl-2,2'-bipyridine\}]Cl_2$ with poly(4-vinylpyridine) in DMF, followed by treatment with hexadecyl bromide or N-(3-bromopropyl)-N'-hexadecyl-4,4'-bipyridinium dibromide. Hydrogen evolution during water photolysis is enhanced and the catalyst particles are

well protected against coagulation[282].

The photolytic dehydrogenation of isopropanol on Pt/TiO_2 catalysts has been studied in the gas and liquid phases[283]. In the gas phase, isopropanol undergoes photodehydrogenation at room temperature in acetone; and in the presence or absence of water vapor, produces an amount of hydrogen equal to the amount of acetone. In the liquid phase, as in the gas phase, the rate of photodehydrogenation increases in the presence of water. Apparently, isopropanol is not a sacrificial compound for reaction in the gas phase; though its role in the liquid phase is yet to be determined[283].

The characteristics of the cathodic deposition of Ag on TiO_2 electrodes under potentiostatic conditions have been established for two different types of electrodes. One TiO_2 electrode was heated at 723K, a high-defect type of electrode; while the other was heated at 1073K, a low-defect electrode[284]. Photoimaging layers of TiO_2 with Ag^+ adsorbed onto the film surface were spectrally sensitized with 1,1'-diethylquino-2,2'-cyanine iodide, chloride or tosylate, or 1,1'-sulfobutyl-2,2'-cyanine betaine. Supersensitization was achieved with 2-(p-dimethylaminostyryl)-benzthiazole[285].

Zinc oxide catalysts mixed with other metal oxides (TiO_2, Al_2O_3) can be prepared by coprecipitation or impregnation techniques, and their activities studied for the decomposition of methanol to synthesis gas[286]. The maximum activity (total conversion of 46 mol%) was observed for a ZnO/TiO_2 catalyst coprecipitated from an aqueous ammonia solution. ZnO/TiO_2 catalysts, prepared *via* hydrolysis of chlorides, were characterized by x-ray photoelectron (XPS) and infrared spectroscopies, along with catalytic elimination reactions of

propanol and butanol[287, 288]. The XPS data suggests the presence of one phase in all the oxides ($ZnTiO_3$), and another phase only in oxides with 64 and 95 mol% ZnO. Infrared-adsorbate spectra of pyridine were indicative of Ti^{4+} cations present on the surface of the $ZnTiO_3$ phase and Zn^{2+} cations present on the surface of the other phase. Active sites for butene isomerization reactions were also examined[288].

The optical properties of ion-beam sputter deposited SiO_2-TiO_2 composite films have been examined with respect to the composition dependence of the optical parameters, the optical energy gap, and the absorption character[289]. Photoelectrochemical properties of p^+-n junction silicon electrodes coated with thin oxide films of titanium, tungsten or iron were examined in aqueous hydrogen iodide and iodine[290]. Effects of the nature of silicon-metal oxide junctions, the donor density in the oxide, the relations between the flatband potential of the oxide and the redox potential of the solution, on the efficiency for solar energy conversion were also discussed. Kulak and Poznyak[291] suggest a charge transfer mechanism to account for the dark conductivity and photoconductivity of n-Si with epitaxial TiO_2 layers in 0.5N K_2SO_4 solutions. The sol-gel process was employed to solve the problem of incorporating an organic dye in an inorganic oxide thin film. Thus, a variety of organic fluorescent dye molecules were embedded in SiO_2 or in SiO_2-TiO_2 films[292]. Absorption and emission spectra were recorded; the data, along with the observed longer lifetimes and energy transfers between trapped dye molecules, and enhanced photostability, correlated with the effects of molecular matrix-isolation on these properties.

Seo and coworkers[293, 294] have studied the reduction of

SO_2 by CO over La_2O_3-impregnated TiO_2, SiO_2 and Al_2O_3. TiO_2-supported catalysts possess good catalytic activity, low COS selectivity, and high La_2O_3 dispersion. Exposure to oxygen during the reaction reduces the catalytic efficiency, though activity is restored when oxygen input is prevented. It would appear that the oxygen lattice vacancy is the active site for the reaction[293].

The activity and selectivity of the commercial catalyst KVTS (vanadium and titanium oxides), and of the newly prepared catalyst K-3, have been examined in relation to the oxidative ammonolysis of 3-picoline[295]. A comparison of the two catalysts reveals the high activity and selectivity of the K-3 catalyst, affording a 90 - 93% yield of nicotinic acid amide and nitrile at total conversion of the starting material 3-picoline. Furthermore, the K-3 catalyst allows for 2-3 fold larger reactor productivity and decreases energy losses[295]. EPR spectroscopy was employed to characterize mechanically-activated TiO_2 and the high-SiO_2 zeolite ZSM-5. For both oxides, O^- hole center associations were detected by a signal at $\lambda = 8$ mm[296].

Photoluminescence studies of TiO_2 anchored onto porous Vycor glass were carried out relative to its photocatalytic activity. Quenching experiment results, interpreted in terms of the x-ray amorphous Ti—O moiety of the catalyst, suggest this moiety to be highly dispersed in the form of an individual complex on the surface. A charge-transfer excited complex explains the results[297].

4.9 COMPLEXES

Pickering[298] has described the preparation and determination of visible and ir spectra, and magnetic moments, of

the $\underline{d}^1$ complex $[Ti(urea)_6]I_3$ specifically for use as a student experiment.

$TiCl_4$ reacts with $(NSCl)_3$ to give $TiCl_4(N_2S_2)$ and $(S_4N_5)_2[Ti_2Cl_{10}]$, the latter of which is shown in Figure 3.

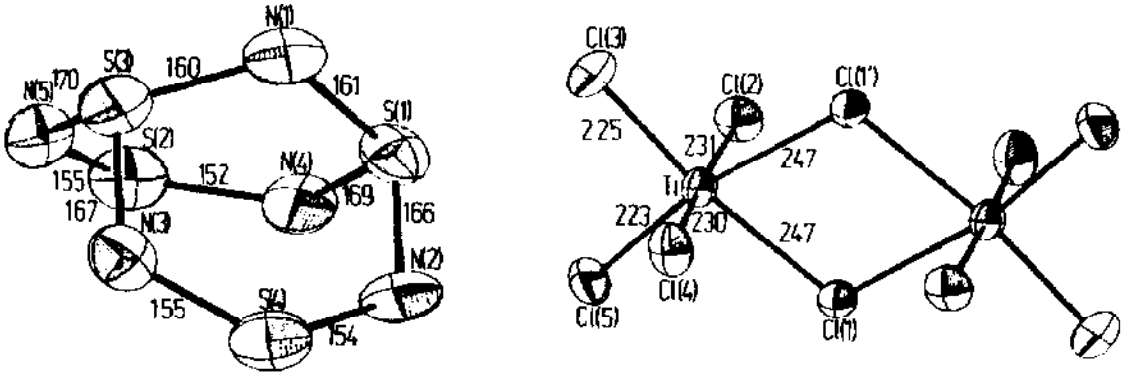

Figure 3. The crystal structure of $(S_4N_5)_2[Ti_2Cl_{10}]$, from reference 299.

According to infrared data, the N_2S_2 ring in $TiCl_4(N_2S_2)$ is bonded to Ti *via* the N atoms. The complex in Figure 3 is composed $S_4N_5^+$ cations, which are nearly equivalent to those in $[S_4N_5]Cl$, and $[Ti_2Cl_{10}]^{2-}$ anions; the latter are nearly identical to those in $(PCl_4)_2[Ti_2Cl_{10}]$[299]. Electronic and ESR spectroscopic studies of titanium(III) thiocyanate complexes indicate that Ti(III) forms distorted tetrahedral and octahedral complexes with thiocyanate ions in ethanol; the two geometric species are in equilibrium. The tetrahedral complex is $Ti(OH)(NCS)_3^-$, wherein the thiocyanate is N-bonded to Ti[300].

Pazos and coworkers[301] have assigned a dimeric structure to $[TiX_4L]$ and a monomeric structure to *cis*-$[TiX_4L_2]$ (X = Cl, Br; L = pyrazole). The preparatory procedure, infrared and Raman

spectra are reported. The preparation and crystal structure of [TiL(THF)Cl] (H_2L = N,N'-ethylenebis(salicylideneimine)) has been cited in the Chinese literature[302]. $TiCl_3 \cdot 3THF$ reacts with Na_2L in THF to afford the air-sensitive [TiL(THF)Cl]; the complex is orthorhombic, belongs to space group Pbnm, and possesses a pseudooctahedral geometry about Ti. Titanyl-acetylacetonate, $[TiO(acac)_2]$, reacts with 1,4,7-triazacyclonone (L) in dry acetone, followed by treatment with aqueous KBr, to give $[Ti_4L_4(\mu\text{-}O)_6]Br_4 \cdot 4H_2O$, as shown in Figure 4. The crystal structure

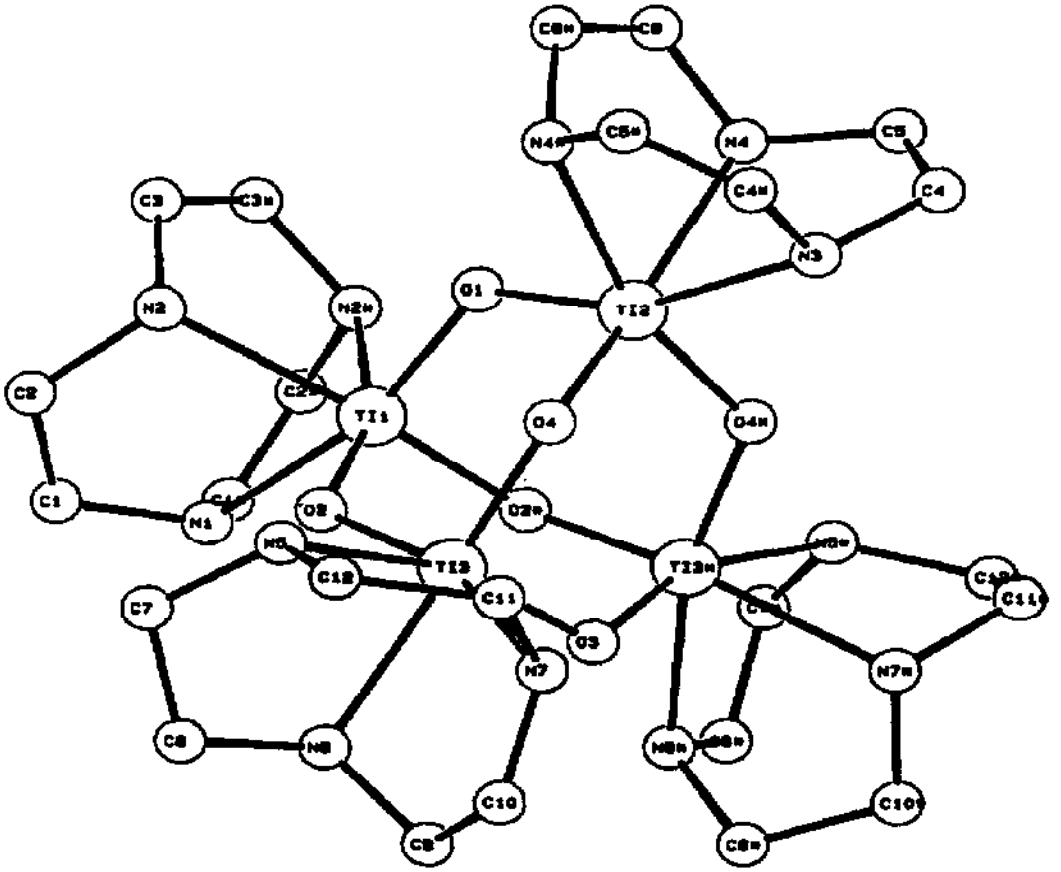

Figure 4. The structure of $[Ti_4(C_6H_{15}N_3)_4(\mu\text{-}O)_6]^{4+}$, in which N(1), Ti(1), O(1), Ti(2), N(3) and O(3) lie on a mirror plane; from reference 303.

determination of this complex reveals the complex to be orthorhombic, space group Pnma, with each Ti atom in a distorted octahedral environment of three facially coordinated N atoms of the L ligand and three cis-μ-oxo groups[303]. Dessy et al.[304] have shown that the reduction of $(NC)_2C=C(CN)_2$ with $Ti(bpy)_3$ (bpy = 2,2'-bipyridine) at 193K in THF and $MeNO_2$ under nitrogen gives the anion in structure (5). This anion can be converted to

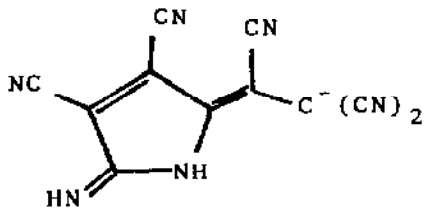

(5)

the Ph_4As^+ salt via treatment with $AsPh_4Cl$ in water. The Russian literature [305] reports the complexing of titanium(IV) with some monoazo compounds based on pyrogallol.

Recent developments in the chemistry of titanium (and vanadium) porphyrins, with special emphasis on oxygen adducts, low valent metalloporphyrins, and related systems with sulfur and selenium, have been reviewed by Guillard and Lecomte[306]. The known crystal structures and reduction of the EXAFS spectra of [Ti(O_2)=TPP] and [Ti(=O)=TPP] (TPP = mesotetraphenylporphyrinato) have been used to ascertain the reliability of a method devised to probe the reality of the peroxide structure of two peroxoiron(III) porphyrinates using EXAFS spectroscopy[307].

2,3-pyridinedicarboxamide reacts in quinoline, with and without $C_6H_3Cl_3$ or pyridine, in the presence of $TiCl_4$ to give $[TiLCl_2]$ (H_2L = tetra-2,3-pyridineporphyrazine). $[TiL(OH)_2]$ forms upon hydrolysis. The complexes were characterized by infrared ad electronic spectra[308].

The crystal structures of $(AsPh_4)_2MCl_5X\cdot 2CH_2Cl_2$ (M = Ti, U, Re, W; X = O, NO, Cl) show the complexes crystallize in three different structure types with essentially equal packing densities. In $(AsPh_4)_2TiCl_6\cdot CH_2Cl_2$, the two $(AsPh_4)^+$ ions are paired around an inversion center such that the three phenyl groups of one ion face three phenyl groups of the other ion in a staggered arrangement; the fourth phenyl group points away from the inversion center. The $(AsPh_4)_2^+$ groupings are aligned to give parallel rows in which contacts between the fourth phenyl groups exist[309].

Titanium(IV) isopropoxide reacts in benzene under nitrogen with salcylideneaniline (HL) to give $[TiL_2(OPr^i)_2]$[310], and with salicylidene-2-aminopyridine (HL') in different stoichiometric ratios to yield $[TiL'_x(OPr^i)_{4-x}]$ (x = 1,2). The latter reaction product may further react with tert-butylalcohol to obtain $[TiL'_x(OBu^t)_{4-x}]$[311].

Sharpless and coworkers[312, 313] have demonstrated that $Ti(OPr^i)_4$ mediates the ring-opening of 2,3-epoxy alcohols and amides with a wide variety of nucleophiles. For example, 3-propyloxiranemethanol reacts under mild conditions with fair to excellent C-3 regioselectivity employing cyanides, halides, thiophenol, selenophenol, thiocyanate, azide, amines, carboxylates, carboxylic acids, p-toluenesulfonate anion, and alcohols as nucleophiles[312].

The β-hydroxy esters $R^1R^2C(OH)CH_2CO_2R$ can be prepared via reaction of ketene $CH_2{=}C{=}O$, R^1COR^2 (R^1 = Or, Me; R^2 = H; $R^1 = R^2$ =

Me), and $Ti(OPr^i)_4$. Polyinsertion of ketene and aldehyde into the Ti—O bonds leads to the di-, tri- and tetra-esters. The presence of excess ketene gives rise to acetyl derivatives of the esters and 6-alkyl-3,4,5,6-tetrahydro-2,4-pyrandiones[314]. In the presence of $Ti(OPr^i)_4$ acting as a catalyst, RSR' (R, R' = p-MeC_6H_4, Me; Ph, Me_3C; p-ClC_6H_4, CH_2CH_2OH; $PhCH_2$, Me) undergoes asymmetric oxidation by tert-butyl hydroperoxide in the presence of (+)-dialkyltartrate to give the chiral sulfoxides RSOR' in good yield. An an example, p-MeC_6H_4SMe is oxidized by Me_3COOH in $ClCH_2CH_2Cl$ at 253K to give a 60% yield of (-)-p-MeC_6H_4SOMe with an enantiomeric excess of 88.3%[315].

Reaction between 1-(trimethylsiloxy)cyclohexene and trans-p-$RC_6H_4CH{=}CHNO_2$ (R = H, Me, MeO, cyano) in CH_2Cl_2 containing a stoichiometric excess of $Ti(OPr^i)_2Cl_2$ at 183K yields the isomeric bicyclic nitronates (6) and (7) with relative preferential ul topicity as primary products[316]. This is

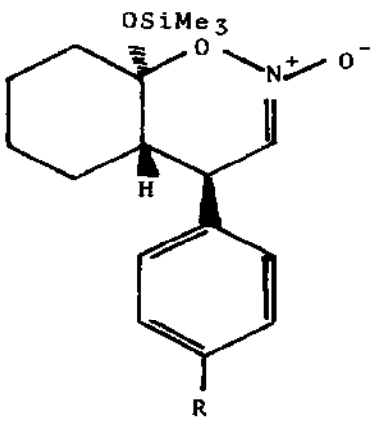

(6)

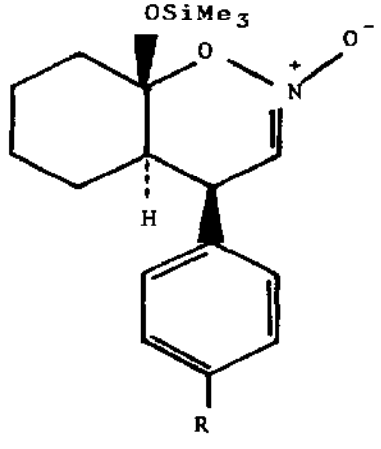

(7)

opposite to that for the corresponding reactions of enolates or enamines. Upon separation of (6) and (7), followed by cleavage with KF-MeOH, 2:1 - 4:1 mixtures of the cyclohexanones (8) and (9) obtain, having like stereochemical topicity. Compound (7) (where

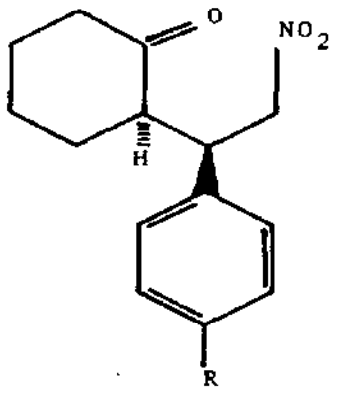

(8)

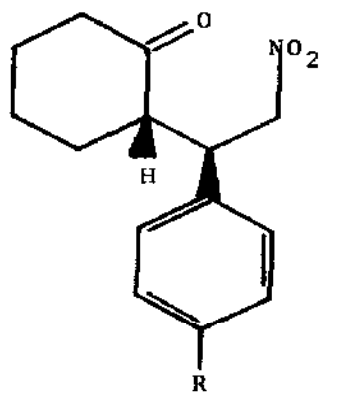

(9)

R = H) additionally yields perhydrobenzopyran (10) via a F^--catalysed nitroaldol addition with PhCHO; the cycloadduct (11) is obtained from a [3 + 2]-dipolar cycloaddition to acrylamide. This

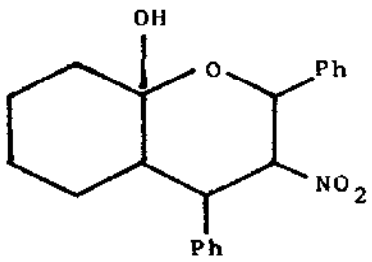

(10)

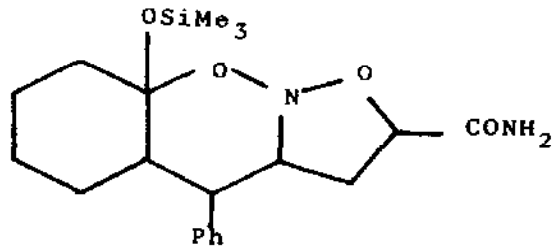

(11)

Michael addition reaction reveals an unlikely stereochemical topicity combination of trigonal centers induced by Lewis acids, which overrides the influence of the donor component configuration [316].

$Ti(OBu)_4$ reacts with unsaturated alcohols to give $[Ti(OBu)_3(OR)]$ (R = $CH_2CH_2OC(O)C(CH_3)=CH_2$, furfuryl, $CH_2C{\equiv}CH$, 2,5-diemthyl-4-(vinylethynyl)-4-piperidyl, $C(CH_3)_2C{\equiv}CCH=CH_2$). The products were characterized by infrared and ^1H nmr spectroscopies [317]. The electronic structure of [pol-$Ti(OBu)_4$ + CH_3OH] has been elucidated by DV-X_α cluster calculations. Substitution of a methoxyl ligand for a butoxyl ligand introduces a characteristic localized state close to the Fermi level; this state may play a crucial role in the photocatalytic decomposition of water[318]. The Russian literature[319] cites the use of $Ti(OBu)_4$ as a catalyst in the transesterification of methylacrylate by butyl alcohol. The reaction involves an exchange of alkoxy groups between methylacrylate and $Ti(OBu)_4$, followed by $Ti(OBu)_4$ regeneration *via* alkoxy exchange with butyl alcohol. The activation energy for the reaction remains constant at 21.3 kcal/mol as methylacrylate concentration increases from 0 - ∞*M*. At 9.5*M* methyl acrylate, the activation energy is 24.5 kcal/mol[319].

Foel[320] has described the synthesis of a monomeric 3-methyl-1-penten-3-oxy derivative of titanium, $Ti[OC(C_2H_5)(CH_3)CH=CH_2]_4$, taking place *via* an alcohol interchange reaction. The complex can also be prepared from the chloride. The complex was characterized by elemental analysis, molecular weight determination, and infrared and ^1H nmr spectra[320].

Titanium tetrachloride reacts with *o*-ClC_6H_4OH in various molar ratios in benzene under different experimental conditions to

yield $Ti(OC_6H_4Cl)_xCl_{4-x}$ (x = 1-4) complexes. The compounds possess a dimeric structure with chlorophenoxy groups acting as bridges[321]. The synthesis and x-ray crystal structure of the sterically demanding phenoxide derivatives of titanium, $Ti\{O\text{-}2,4,6\text{-}\underline{tert}\text{-}Bu)_3C_6H_2\}_2(NMe_2)_2$, have been reported by Jones <u>et al</u>.[322]. The catalytic activity of the $PhOTiCl_3$-$AlEt_2Cl$ system for the polymerization of ethylene has been studies; the EPR spectrum shows a signal characterizing the reduction of Ti^{4+} to Ti^{3+}. Both the activity and the EPR signal increas on increasing the Al/Ti molar ratio to 1.75. However, at a molar ratio > 1.75, the EPR signal reamins constant while the activity of the complexes decreases. The optimum reaction parameters include an Al/Ti molar ratio of 1.5 - 1.85, a reaction temperature of 303 - 313K, reaction times of 15 minutes, and a Ti concentration in the complex of 0.15 - 0.20 molTi/liter[323].

The preparation, and physical and spectral characterization of the β-diketonate complexes $TiCl_2L_2$ (HL = benzoylacetone, dibenzoylmethane, <u>p</u>-methoxybenzoylacetone, <u>p</u>-chlorobenxoylacetone) have been re-examined by Sun and Ren[324]. These air-stable, water insoluble complexes readily undergo hydrolysis in aqueous organic solvents with the formation of a TiO_2 precipitate, and exhibit some antitumor properties. The mass spectrum of the dimer of titanyl acetylacetonate has been reported[325] and discussed in terms of the dissociation of odd and even neutral fragments. The intensity of ions arising from the dimer is relatively higher than that from ions due to the polymerization of other metal acetylacetonates in the vapor phase. The β-diketonate complex $[Ti(acac)_3]_2TiCl_6$ (acac = acetylacetonate) has been employed as an oxidation catalyst for cyclohexane in the liquid phase[326]. Poluboyarov and coworkers[327] have carried out ESR studies on the

titanium(3+) complexes formed in the catalytic system ($Ti(acac)_2Cl_2$ + Et_2AlCl) for homogeneous polymerization. Also investigated were the changes in coordination state of Ti^{3+} upon interaction with ethylene, carbon monoxide, and pyridine. Reaction of substituted o-benzoquinones with TiF_4 (and SnF_4) yields TiF_3L (and SnF_3L) (HL = o-semiquinone). ESR results suggest a trigonal bipyramidal structure for TiF_3L in nonpolar solvents, and an octahedral structure in polar solvents for TiF_3LS (S = organic solvent)[328].

Ogino[329] has reviewed the unusually rapid substitution reaction rates of metal(III)-EDTA complexes, where M(III) is Ti(III), Cr(III), Fe(III), Os(III), and Ru(III). The rapid rates are probably the result of the mediation of transient seven-coordinate structures in solution. The kinetics of the reduction of $[Ru_2(OAc)_2(C_2O_4)_2(H_2O)_2]^-$ by Ti(HEDTA) show several distinct stages[330]. The first stage is a substitution reaction giving rise to a multinuclear intermediate. The second stage involves a rate-limiting electron transfer reaction within the assembled multinuclear complex. Subsequent slower stages correspond to the breakup of the multinuclear Ru(II)$_2$—Ti(IV) complex formed by electron transfer[330].

Rodriguez and coworkers[331] have prepared and characterized (infrared and ^1H nmr spectroscopies) the cis-$TiCl_4(HL)_2$ complexes (HL = $RC_6C_4CH{=}NC_6H_4OH$-o; R = H, 2-Cl, 4-Cl, 2-OMe, 4-OMe, 4-Me, 4-NO_2). The ligands appear to be monodentate and bonded to Ti through the phenolic oxygen atom. Good yields of high-purity $TiO(HL)_2 \cdot 2H_2O$ (H_2L = L-ascorbic acid) have been obtained[332].

Octahedral TiX_4L (L = dithiooxamide; X = Cl, Br) complexes can be prepared via addition of L in CH_2Cl_2 to TiX_4 under dry and inert conditions. Electronic, infrared and UV spectra, and

conductivity data indicate coordination through the S atom of the C-S group[333]. The same authors[334] have prepared $TiX_4 \cdot TEDTO$ (TEDTO = tetraethyldithiooxamide; X = Br, Cl) by a similar reaction. Spectral characterization (electronic, infrared, UV) and conductivity data indicate coordination *via* the thiocarbonyl S atom, with the most likely structure being octahedral with the TEDTO ligand in the *cis* position[334]. The preparation and characterization of TiL_4 (HL = 5-aminoindazolyl dithiocarbamic acid) was reported by Kureshy *et al.*[335]. The infrared spectral results were interpreted in terms of octahedral structures in which two of the dithiocarbamate moieties are bound symmetrically and two others are bound unsymmetrically to the metal ion.

ACKNOWLEDGEMENTS

Our work is generously supported by the National Sciences and Engineering Council of Canada and by the North Atlantic Treaty Organization (No. 843/84). We thank these agencies for their support.

REFERENCES

1. a) To whom correspondence should be addressed; Chemistry Department, Concordia University, Montreal, Quebec, Canada H3G 1M8. b) Chemistry Department, Concordia University, Montreal, Quebec, Canada H3G 1M8. c) Istituto di Chimica Analitica, Universita di Torino, 10126 Torino, Italia.
2. B.I. Nabivanets, V.G. Matyashev and N.V. Chernaya, Zh. Anal. Khim., 39 (1984) 1733.
3. A.K. Sharma and N.K. Kaushik, Thermochim. Acta, 83 (1985) 347.
4. S. Hayashi, Kagaku Kogyo Shiryo, 19 (1985) 166.
5. N.A. Vasyutinskii, Izv. Akad. Nauk SSSR, Neorg. Mater., 54 (1985) 54.
6. N.R. Bukeikhanov, B.V. Suvorov and B.T. Dzhusupov, Izv. Akad. Nauk Kaz. SSR, Ser. Khim., (1985) 51.
7. J. Lafait, Vide, Couches Minces, 39 (1984) 299.
8. A.L. Ivanovskii, V.A. Gubanov and E.Z. Kurmaev, J. Phys.

Chem. Solids, 46 (1985) 823.
9. B. Nowak and M. Minier, J. Less-Common Met., 101 (1984) 245.
10. R.C. Bowman, Jr., B.D. Craft, W.E. Tadlock, E.L. Venturini and J.S. Cantrell, J. Appl. Phys., 57 (1985) 3036.
11. H. Yayama, K. Hirakawa and A. Tomokiyo, KOgaku Shuho-Kyushu Daigaku, 58 (1985) 139.
12. See reference 11 and references therein.
13. J. Klima, G. Schadler, P. Weinberger and A. Neckel, J. Phys. F, 15 (1985) 1307.
14. K. Uchida and B. Kyoh, Kinki Daigaku Rikogakubu Kenkyu Hokoku, (1984) 393.
15. A. El Jazouli, A. Serghini, R. Brochu, J.M. Dance and G. Le Flem, C.R. Acad. Sci., Ser. 2, 300 (1985) 493.
16. W.M. Theis, G.B. Norris and M.D. Porter, Appl. Phys. Lett., 46 (1985) 1033.
17. G. Blasse, G.J. Dirksen and L.H. Brixner, Mater. Res. Bull., 20 (1985) 989.
18. S.N. Patel and A.A. Balchin, J. Mater. Sci. Lett., 3 (1984) 942.
19. K. Kanehori, F. Kirino, K. Miyauchi and T. Kudo, Denki Kagaku oyobi Kogyo Butsuri Kagaku, 53 (1985) 287.
20. L. Bernard, M. McKelvy, W. Glaunsinger and P. Colombet, Solid State Ionics, 15 (1985) 301.
21. S.N. Patel and A.A. Balchin, J. Mater. Sci., 20 (1985) 917.
22. R. Schoellhorn and A. Payer, Angew. Chem., 97 (1985) 57.
23. K.O. Klepp, Z. Naturforsch., B:Anorg. Chem., Org. Chem., 40B (1985) 229.
24. G.A. Wiegers, H.J.M. Bouwmeester and A.G. Gerards, Solid State Ionics, 16 (1985) 155.
25. M. Inoue and H. Negishi, J. Phys. Soc. Jpn., 54 (1985) 380.
26. P. Choudhury, B. Ghosh, M.B. Patel and H.D. Bist, J. Raman Spectrosc., 16 (1985) 149.
27. P. Choudhury, B. Ghosh, M.B. Patel and H.D. Bist, J. Phys. C, 17 (1984) 5827.
28. P. Choudhury, B. Ghosh and H.D. Bist, Proc. Nucl. Phys. Solid State Phys. Symp., 1982, 25C (1984) 465.
29. A.N. Das, P. Choudhury and B. Ghosh, J. Phys. C: Solid State Phys., 18 (1985) 5975.
30. P. Choudhury, B. Ghosh and H.D. Bist, Proc. Nucl. Phys. Solid State Phys. Symp., 1982, 25C (1984) 45.
31. H.M. Cheung and R.L. Lichti, J. Phys. C: Solid State Phys., 18 (1985) 6157.
32. M.K. Chaudhuri and B. Das, Polyhedron, 4 (1985) 1449.
33. G. Pausewang and R. Schmidt, Z. Anorg. Allg. Chem., 523 (1985) 213.
34. T.C. DeVore and T.N. Gallaher, J. Chem. Phys., 82 (1985) 2512.
35. T.E. Jenkins, J. Raman Spectrosc., 15 (1984) 308.
36. N.V. Galitskii, N.K. Evseev, E.P. Medvedchikov and V.I. Starshenko, Titanium: Sci. Technol., Proc. Int. Conf. Titanium, 5th,1984, 1 (1985) 97.
37. G. Meyer and U. Packruhn, Z. Anorg. Allg. Chem., 524 (1985) 90.
38. D. Gordon and M.G.H. Wallbridge, Inorg. Chim. Acta, 88 (1984) 15.
39. V.I. Shapoval, V.F. Grishchenko, L.I. Zarubitskaya, V.G. Lutsenko and V.V. Nerubashchenko, Fiz. Khim. Elektrokhim. Redk. Met. Solevykh Rasplavakh, (1984) 9.
40. K. Hallmeier, E. Hartmann and R. Szargan, Wiss. Z.-Karl-Marx-Univ. Leipzig, Math.-Naturwiss. Reihe, 33 (1984) 382.

41. K.G. Ravikumar, S. Gunawekaran and S. Mohan, Acta Phys. Pol., A, A67 (1985) 1129.
42. S.I. Kulichenko, Yu.A. Byval'tsev, and B.G. Perelygin, Probl. Kalorim. Khim. Termodin., Dokl. Vses. Konf., 10th, 1 (1984) 297.
43. S.I. Troyanov and G.N. Mazo, Vestn. Mosk. Univ., Ser. 2:Khim., 25 (1984) 606.
44. S.I. Troyanov, G.N. Mazo and M.A. Simonov, Koord. Khim., 11 (1985) 1147.
45. P. Sobota and Z. Janas, J. Organomet. Chem., 276 (1984) 171.
46. V. Kh. Dobruskin, S.E. Kurashvili and S.I. Kol'tsov, Zh.Fiz. Khim., 59 (1985) 781.
47. V.A. Reznichenko, F.B. Khalimov and T.B. Goncharenko, Deposited Doc. (1983), VINITI 6765-83, 12pp.
48. L. Ciavatta, D. Ferri and G. Riccio, Polyhedron, 4 (1985) 15.
49. S. Ya. Kuchmii, A.V. Korzhak and A.I. Kryukov, Koord. Khim., 10 (1984) 1505.
50. J.R. Masaguer and M.A. Mendiola, Transition Met. Chem., 10 (1985) 243.
51. K. Siddiqi, N.H. Khan, R.I. Kureshy, L.A. Khan, S. Tabassum and S.A.A. Zaidi, Indian J. Chem., Sect. A, 24A (1985) 68.
52. I. Rosca and M. Temiciuc, Izv. Khim., 17 (1984) 239.
53. R. Ran, S. Jiang and J. Shen, Yingyong Huaxue, 2 (1985) 29.
54. Yu.G. Yatluk and A.L. Suvorov, Zh. Prikl. Khim. (Leningrad), 58 (1985) 1824.
55. A. Clerici and O. Porta, J. Org. Chem., 50 (1985) 76.
56. G. Maier, R.K. Schmitt and U. Seipp, Chem. Ber., 118 (1985) 722.
57. T. Takeda, T. Tsuchida and T. Fujiwara, Chem. Lett., (1984) 1219.
58. H.U. Reissig and I. Reichelt, Tetrahedron Lett., 25 (1984) 5879.
59. B. Venugopalan, S.S. Iyer and N.J. De Souza, Heterocycles, 23 (1985) 1425.
60. G.S. Bikushev, Kinet. Katal., 25 (1984) 1323.
61. G. Guo, Y. Xie and Y. Tang, Wuli Huaxue Xuebao, 1 (1985) 57.
62. L.A. Yatsenko, A.G. Boldyrev, I.G. Zhuchikhina, S.V. Ivanova and E.N. Kropacheva, Kinet. Katal., 26 (1985) 244.
63. J.Y. Tsao and D.J. Ehrlich, J. Chem. Phys., 81 (1984) 4620.
64. J.C. Ewing, G.S. Ferguson, D.W. Moore, F.W. Schultz and D.W. Thompson, J. Org. Chem., 50 (1985) 2124.
65. O.H. Ellestad, J. Mol. Catal., 31 (1985) 119.
66. N. Kashiwa adn J. Yoshitake, Polym. Bull. (Berlin), 12 (1984) 99.
67. R. Spitz, J.L. Lacombe and A. Guyot, J. Polym. Sci., Polym. Chem. Ed., 22 (1984) 2641.
68. R. Spitz, J.L. Lacombe and A. Guyot, J. Polym. Sci., Polym. Chem. Ed., 22 (1984) 2625.
69. N. Kashiwa, A. Mizuno and S. Minami, Polym. Bull. (Berlin), 12 (1984) 105.
70. N. Kashiwa, T. Tsutsui and A. Toyota, Polym. Bull. (Berlin), 12 (1984) 111.
71. S.I. Troyanov, G.N. Mazo and M.A. Simonov, Vestn. Mosk. Univ., Ser. 2: Khim., 25 (1984) 458.
72. W. Brendel, T. Samartzis, C. Brendel and B. Krebs, Thermochim. Acta, 83 (1985) 167.
73. A.N. Cormack, C.M. Freeman, R.L. Royle and C.R.A. Catlow, Mater. Sci. Monogr., 28A(React. Solids, Pt. A) (1985) 321.
74. K.E. Smith and V.E. Henrich, Phys. Rev. B: Condens. Matter, 32 (1985) 5384.

75. G.A. Zenkovets and D.V. Tarasova, Izv. Sib. Otd. Akad. Nauk SSSR, Ser. Khim. Nauk, (1984) 42.
76. S.V. Chernousov and N.V. Tolstoguzov, Fiz.-Khimiya i Tekhnol. Dispers. Poroshkov, Kiev, (1984) 11.
77. L.A. tarasov, S.V. Morozov, A.V. Sharkov and G.V. Logunova, Geterogen. Katalitich. Protsessy, L., (1984) 103.
78. H. Harada, H. Kanno and T. Ueda, Denki Kagaku oyobi Kogyo Butsuri Kagaku, 53 (1985) 736.
79. Y. Morita, Kenkyu Hobun-Asahikawa Kogyo Koto Senmon Gakko, 22 (1985) 123.
80. H. Kanno, Y. Yamamoto and H. Harada, Chem. Phys. Lett., 121 (1985) 245.
81. S. Nishimoto, B. Ohtani, H. Kajiwara and T. Kagiya, J. Chem. Soc., Faraday Trans. I, 81 (1985) 61.
82. J. Abrahams, R.S. Davidson and C.L. Morrison, J. Photochem., 29 (1985) 353.
83. F.R.F. Fan, H.Y. Liu and A.J. Bard, J. Phys. Chem., 89 (1985) 4418.
84. V.I. Zarko, E.G. Sivalov, G.M. Kozub and A.A. Chuiko, Dopov. Akad. Nauk Ukr. RSR, Ser. B: Geol., Khim. Biol. Nauki, (1985) 37.
85. G. Busca, P. Forzatti, J.C. Lavalley and E. Tronconi, Stud. Surf. Sci. Catal., 20(Catal. Acids Bases) (1985) 15.
86. A.G. Shastri, A.K. Datye and J. Schwank, Appl. Catal., 14 (1985) 119.
87. M.G. Blanchin, L.A. BUrsill and D.J. Smith, Phys. Status Solidi A, 89 (1985) 559.
88. M.G. Blanchin and L.A. Bursill, Phys. Status Solidi A, 86 (1984) 101.
89. R.L. Crackel and W.S. Struve, Chem. Phys. Lett., 120 (1985) 473.
90. S.V. Vosel, E.E. Pomoshchnikov, V.A. Poluboyarov and V.F. Anufrienko, Kinet. Katal., 25 (1984) 1501.
91. G.A. Zenkovets, I.P. Olen'kova, D.V. Tarasova, F.S. Gadzhieva, I.A. Ovsyannikova, V.F. Anufrienko and V.I. Iskorskii, Izv. Akad. Nauk SSSR, Neorg. Mater., 20 (1984) 1526.
92. M. Graetzel and F.P. Rotzinger, Chem. Phys. Lett., 118 (1985) 474.
93. L.S. Hsu, R. Solanki, G.J. Collins and C.Y. She, Appl. Phys. Lett., 45 (1984) 1065.
94. C. Braun and J.C. Andre, J. Photochem., 28 (1985) 13.
95. J.F. Marucco, B. Poumellec, J. Gautron and P. Lemasson, J. Phys. Chem. Solids, 46 (1985) 709.
96. G. Busca, H. Saussey, O. Saur, J.C. Lavalley and V. Lorenzelli Appl. Catal., 14 (1985) 245.
97. B. Babuji and S. Radhakrishna, J. Mater. Sci. Lett., 4 (1985) 767.
98. G.B. Raupp and J.A. Dumesic, J. Phys. Chem., 89 (1985) 5240.
99. A.A. Tsyganenko, L.A. Denisenko, S.M. Zverev and V.N. Filimonov, J. Catal., 94 (1985) 10.
100. V.B. Gusev, D.G. Kleshchev and I.I. Kalinichenko, Zh. Prikl. Khim. (Leningrad), 58 (1985) 33.
101. D.G. Kleshchev, R.N. Pletnev, V.Yu. Pervushin, R.A. Denisova and A.V. Tolchev, Kvant. Khimiya i Radiospektroskopiya Tverd. Tela, Sverdlovsk, (1984) 48.
102. V.Yu. Perushin, T.A. Denisova, A.V. Tolchev, V.P. Marchenko, R.N. Pletnev, V.A. Tyustin and D.G. Kleshchev, Zh. Neorg. Khim., 30 (1985) 855.

103. R.L. Sasseville, S. MAmiche-Afara, M.F. Weber and M.J. Dignam, Adv. Hydrogen Energy, 4(Hydrogen Energy Prog. 5, Vol. 3) (1984) 1047.
104. Y. Barakat, E.A. Garcia and C. Coddet, Mater. Sci. Monogr., 28A(React. Solids, Pt. A) (1985) 215.
105. L. Parent, J.P. Dodelet, G.G. Ross, B. Terreault and S. Dallaire, J. Electrochem. Soc., 132 (1985) 2590.
106. V.I. Zarko, G.M. Kozub, L.S. Antonova, V.V. Pavlov and A.A. Chuiko, Ukr. Khim. Zh. (Russ. Ed.) 50 (1984) 1060.
107. A. Roy, S.S. Bhattacharyya and S. Aditya, Trans. SAEST, 19 (1984) 185.
108. A. Roy, S.S. Bhattacharyya and S. Aditya, Adv. Hydrogen Energy, 4(Hydrogen Energy Prog. 5, Vol. 3) (1984) 1003.
109. Y. Aikawa, T. Sagara and M. Sukigara, Denki Kagaku Oyobi Kogyo Butsuri Kagaku, 53 (1985) 638.
110. H.S. Jarrett, Phys. Rev. Lett., 54 (1985) 217.
111. K.J. Hartig, G. Grabner, N. GEtoff, G. Popkirov and S. Kanev, Ber. Bunsen-Ges. Phys. Chem., 89 (1985) 831.
112. W.J. Albery, P.N. Bartlett and J.D. Porter, J. Electrochem. Soc., 131 (1984) 2896.
113. W. Smit, J. Electrochem. Soc., 132 (1985) 2172.
114. Y. Yonezawa, R. Hanawa and H. Hada, J. Imaging Sci., 29 (1985) 171.
115. Y. Nakato and H. Tsubomura, J. Photochem., 29 (1985) 257.
116. Y. Shi, X.R. Dai, Q. Gao and B. Sun, Yingyong Kexue Xuebao, 2 (1984) 361.
117. C. Gutierrez and P. Salvador, J. Electroanal. Chem. Interfacial Electrochem., 187 (1985) 139.
118. A. Viehbeck and E.W. DeBerry, J. Electrochem Soc., 132 (1985) 1369.
119. H. Masuda, N. Shimidzu and S. Ohno, Denshi Shashin Gakkaishi, 24 (1985) 27.
120. V. Antonucci, E. Passalacqua, P.L. Antonucci and N. Giordano, Int. J. Hydrogen Energy, 10 (1985) 585.
121. Kh.Z. Brainina, M.Ya. Khodos, G.M. Belysheva and N.V. Krivosheev, Elektrokhimiya, 20 (1984) 1380.
122. F. Beck and W. Gabriel, Angew. Chem., 97 (1985) 765.
123. R.E. Hetrick, Appl. Phys. Commun., 5 (1985) 177.
124. E. Serwicka, Colloids Surf., 13 (1985) 287.
125. A. Sh. Aliev, A.I. Aledperov, V.P. Pakhomov and V.N. Fateev, Elektrokhimiya, 21 (1985) 370.
126. T. Sekine, H. Ueda and M. Yonemura, Nippon Kagaku Kaishi, (1985) 1024.
127. Y. Inoue, M. Ikamura and K. Sato, J. Phys. Chem., 89 (1985) 5184.
128. P. Salvador and F. Decker, J. Phys. Chem., 88 (1984) 6116.
129. P. Salvador, J. Phys. Chem., 89 (1985) 3863.
130. V. Rives-Arnau, J. Electroanal. Chem. Interfacial Electrochem., 190 (1985) 279.
131. H. Muraki, T. Saji, M. Fugihira and S. Aoyagui, J. Electroanal. Chem. Interfacial Electrochem., 169 (1984) 319.
132. F.V. Kerchove, A. Praet and W.P. Gomes, J. Electrochem. Soc., 132 (1985) 2357.
133. K. Kalyanasundaram and M. Graetzel, Report (1984), EUR-9273-EN, 28 pp, Abstr. No. 18070.
134. E. Amouyal and P. Koffi, J. Photochem., 29 (1985) 227.
135. M. Neumann-Spallart and O. Enea, J. Electrochem. Soc., 131 (1984) 2767.
136. O. Enea, Nouv. J. Chim., 9 (1985) 281.

137. D. Bahnemann, A. Henglein and L. Spanhel, Faraday Discuss. Chem. Soc., 78 (1984) 151.
138. M. Dardoux, D. Klvana, M. Duran and M. Bideau, Can. J. Chem., 63 (1985) 668.
139. V.I. Stepanenko, L.V. Lyashenko and V.M. Belousov, Khim. Fiz., 4 (1985) 97.
140. K. Takagi, T. Fujioka and Y. Sawaki, Chem. Lett., (1985) 913.
141. I. Mochida, Y. Iwai, T. Kamo and H. Fujitsu, J. Phys. Chem., 89 (L985) 5439.
142. M.A. Fox and T.L. Pettit, J. Org. Chem., 50 (1985) 5013.
143. See reference 142 and references therein.
144. T.L. Rose and C. Nanjundiah, J. Phys. Chem., 89 (1985) 3766.
145. Y. Matsumoto, Y. Yamaguchi and E. Sato, Bull. Chem. Soc. Japan, 58 (1985) 1255.
146. I. Wang, J.C. Wu and C.S. Chung, Appl. Catal., 16 (1985) 89.
147. L. Heinrich, Chem.-Ing.-Tech., 56 (1984) 646.
148. B. Ohtani, J. Handa, S. Nishimoto and T. Kagiya, Chem. Phys. Lett., 120 (1985) 292.
149. P.V. Kamat, J. Chem. Soc., Faraday Trans. 1, 81 (1985) 509.
150. J.D. Brown, D.L. Williamson and A.J. Nozik, J. Phys. Chem., 84 (1985) 3076.
151. M. Anpo, N. Aikawa, Y. Kubokawa, M. Che, C. Louis and E. Giamello, J. Phys. Chem., 89 (1985) 5689.
152. E. Borgarello, E. Pelizzetti, R. Balardini and F. Scandola, Nouv. J. Chim., 8 (1984) 567.
153. D. Bahnemann, A. Henglein, J. Lilie and L. Spanhel, Vortragstag. Fachgruppe Photochem.[Ges. Dtsch. Chem.], 8th, (1983) 145.
154. H.Q. Dao and F. Pruchnik, Pol. J. Chem., 58 (1984) 823.
155. H.Q. Dao and F. Pruchnik, Pol. J. Chem., 58 (1984) 817.
156. F. Solymosi, I. Tombacz and J. Koszta, J. Catal., 95 (1985) 578.
157. M.Y. He, J.M. White and J.G. Ekerdt, J. Mol. Catal., 30 (1985) 415.
158. K. Okamoto, Y. Yamamoto, H. Tanaka, M. Tanaka and A. Itaya, Bull. Chem. Soc. Japan, 58 (1985) 2015.
159. K. Okamoto, Y. Yamamoto, H. Tanaka and A. Itaya, Bull. Chem. Soc. Japan, 58 (1985) 2023.
160. H. Fukui, M. Tanaka and Y. Fujiyama, Shikizai Kyokaishi, 57 (1984) 487.
161. J. Novrocik, J. Norek and M. Novrocikova, Chem. Prum., 35 (1985) 31.
162. T.A. Denisova, R.N. Pletnev, L.A. Perelyaeva and M.P. Tsvetkova, Deposited Doc., (1983) VINITI 4280-83, 20 pp.
163. A.A. Dvernyakova, G.N. Novitskaya and M.V. Verkhovskaya, Izv. Akad. Nauk SSSR, Neorg. Mater., 21 (1985) 442.
164. S. Suzuki, N. Horiuchi and Y. Hori, Kankyo Kagaku Kenkyu Hokoku (Chiba Daigaku), 1983, 9 (Pub. 1984) 24.
165. T. Ibusuki and K. Takeuchi, Taiki Osen Gakkaishi, 20 (1985) 82.
166. H. Courbon and P. Pichat, J. Chem. Soc., Faraday Trans. 1, 80 (1984) 3175.
167. M. Malinowski, R. Dams and H.J. Geise, Bull. Soc. Chim. Belg., 94 (1985) 93.
168. G. Mink, I. Bertoti, I.S. Pap, T. Szekely, C. Battistoni and E. Karmazsin, Thermochim. Acta, 85 (1985) 83.
169. K. Itaya, I. Uchida, S. Toshima and R.M. De la Rue, J. Electrochem. Soc., 131 (1984) 2086.

170. T. Mitsuhashi and Y. Fujiki, Thermochim. Acta, 88 (1985) 177.
171. R. Werthmann and R. Hoppe, Z. Anorg. Allg. Chem., 519 (1984) 117.
172. M.R. Balasubramanian, J. Indian Chem. Soc., 62 (1985) 323.
173. L.P. Sonntag and M.T. Spitler, J. Phys. Chem., 89 (1985) 1453.
174. K.H. Yoon, T.H. Kim, Yoop Hakhoechi, 22 (1985) 19.
175. Yu.V. Pleskov, M.D. Krotova and A.A. Revina, Radiat. Phys. Chem., 26 (1985) 17.
176. V. Balek and E. Kaisersberger, Thermochim. Acta, 85 (1985) 207.
177. B.I. Nabivanets and Yu.A. Omel'chenko, Zh. Prikl. Khim., (Leningrad), 58 (1985) 2110.
178. T.R.N. Kutty and L.G. Devi, Mater. Res. Bull., 20 (1985) 793.
179. P. Pononis and J.C. Vickerman, J. Catal., 90 (1984) 305.
180. M. Herrero-Fernandez, J.M. Gonzalez-Calbet and M.A. Alario-Franco, Thermochim. Acta, 85 (1985) 79.
181. L.N. Matyushina and A.I. Vorobeichik, Zh. Neorg. Khim., 30 (1985) 1954.
182. I.A. Topol and N.G. Rambidi, Chem. Phys., 92 (1985) 299.
183. T.B. Zunic, S. Scavnicar and Z. Grobenski, Croat. Chem. Acta, 57 (1984) 645.
184. I.E. Wachs, S.S. Chan and C.C. Chersich, Mater. Sci. Monogr., 28B(React. Solids, Pt. B) (1985) 1047.
185. G. Busca, L. Marchetti, G. Centi and F. Trifiro, J. Chem. Soc., Faraday Trans. 1, 81 (1985) 1003.
186. L. Rey, R. Martino, L.A. Gambaro and H.J. Thomas, Actas Simp. Iberoam. Catal., 9th, 2 (1984) 1463.
187. I.E. Wachs and S.S. Chan, Appl. Surf. Sci., 20 (1984) 181.
188. I.A. Vasil'eva and G.S. Suleimenova, Dokl. Akad. Nauk SSSR, 278 (1984) 904 [Phys. Chem.].
189. M. Rusiecka, Ser. Fiz. (Uniw. im. Adama Mickiewicza Poznaniu), 53(Radio Microwave Spectrosc.) (1985) 265.
190. R. Haase, U. Illgen, J. Scheve and I.W. Schulz, React. Kinet. Catal. Lett., 28 (1985) 395.
191. A. Andersson and S.L.T. Andersson, ACS Symp. Ser., 279(Solid State Chem. Catal.) (1985) 121.
192. C. Otero-Diaz, M.A. Alario-Franco, An. Quim., Ser. B, 79(3, Suppl. 1) (1983) 510.
193. E.N. German, V.I. Bashin and E.M. Guseinov, Khim.-Farm. Zh., 19 (1985) 592.
194. L.N. Raevskaya and Yu.I. Pyatnitskii, React. Kinet. Catal. Lett., 26 (1984) 173.
195. N.R. Bukeikhanov, P.B. Vorob'ev, B.V. Suvorov, A.G. Lyubarskii, A.G. Gorelik, A.S. Zulkasheva, L.F. Gabdullina, E.V. Ivanov and L.A. Stepanova, Izv. Akad. Nauk Kaz. SSR, Ser. Khim., (1985) 58.
196. J. Skrzypek, M. Grzesik, M. Galantowicz and J. Solinski, Chem. Eng. Sci., 40 (1985) 611.
197. I.E. Wachs, R.Y. Saleh, S.S. Chan and C.C. Chersich, Appl. Catal., 15 (1985) 339.
198. A. Sobczynski and J.M. White, J. Mol. Catal., 29 (1985) 379.
199. F. Beck and H. Schulz, Electrochim. Acta, 29 (1984) 1569.
200. E. Bordes, S.J. Jung and P. Courtine, Actas Simp. Iberoam. Catal., 9th, 2 (1984) 983.
201. Y.C. Liu, G.L. Griffin, S.S. Chan and I.E. Wachs, J. Catal., 94 (1985) 108.
202. Y. Sun and Y. Ding, Cuihua Xuebao, 5 (1984) 228.
203. L.L. Murrell and R.L. Garten, Appl. Surf. Sci., 19 (1984) 218.

204. D. Cordischi, N. Burriesci, F. D'Alba, M. Petrera, G. Polizzotti and M. Schiavello, J. Solid State Chem., 56 (1985) 182.
205. L. Tau andC.O. Bennett, J. Catal., 89 (1984) 327.
206. D. Brugniau, S.D. Parker and G.E. Rhead, Thin Solid Films, 121 (1984) 247.
207. J.S. THorp and H.S. Eggleston, J. Mater. Sci., 20 (1985) 2369.
208. M.I. Yanovskaya, Yu.E. Roginskaya, N.V. Kolganova, M.A. Sevost'yanov, E. Lubnin, I.M. Yanovskaya and O.L. Lependina, Poverkhnost, (1985) 115.
209. N. Wagner and O. Bruemmer, Phys. Status Solidi A, 89 (1985) K123.
210. T. Kishi, Denki Kagaku oyobi Kogyo Butsuri Kagaku, 53 (1985) 453.
211. M. Valigi, D. Cordischi, D. Gazzoli, K.P. Keijzers and A.A.K. Adri, J. Chem. Soc., Faraday Trans. 1, 81 (1985) 813.
212. H. Bartelt, Wiss. Z. Humboldt-Univ. Berlin, Math.-Naturwiss. Reihe, 34 (1985) 50.
213. F. Hine, M. Yasuda, T. Iida, Y. Ogata and K. Hara, Electrochim. Acta, 29 (1984) 1447.
214. N. Wagner and O. Bruemmer, Beitr. Tag. Mikrosonde. 6th. (1984) 213.
215. K.W. Blazey, K.A. Mueller, W. Berlinger, P. Triggs and F. Levy, Solid State Commun., 54 (1985) 1039.
216. A.A. Uzbekov and V.S. Klement'eva, Elektrokhimiya, 21 (1985) 758.
217. V.S. Klement'eva and A.A. Uzbekov, Elektrokhimiya, 21 (1985) 796.
218. G. Gusinskii, V.I. Ignat'ev, N.V. Makarenko, L.A. Rassadin and S.P. Chernova, Zavad. Lab., 50 (1984) 27.
219. V.S. Klement'eva, A.A. Uzbekov, V.L. Kubasov and V.G. Lambrev, Zh. Prikl. Khim. (Leningrad), 57 (1984) 2623.
220. A.A. Uzbekov, V.S. Klement'eva, V.L. Kubasov and V.G. Lambrev, Zh. Prikl. Khim. (Leningrad), 58 (1985) 686.
221. Z. Quan and H. Yen, Gaodeng Xuexiao Huaxue Xuebao, 6 (1985) 451.
222. D.V. Kokoulina and L.V. Bunakova, Elektrokhimiya, 20 (1984) 1481.
223. N.Ya. Bune, E.N. Perminova and V.V. Losev, Elektrokhimiya, 20 (1984) 1561.
224. N.Ya. Bune, M.Yu. Portnova, V.P. Filatov and V.V. Losev, Elektrokhimiya, 20 (1984) 1291.
225. D.V. Kokoulina, L.V. Bunakova and M.Z. Eleva, Elektrokhimiya, 21 (1985) 1121.
226. R.G. Erenburg, Elektrokhimiya, 20 (1984) 1602.
227. S.R. Morris, R.B. Moyes, P.B. Wells and R. Whyman, J. Catal., 96 (1985) 23.
228. Y. Udagawa, K. Tohji, A. Ueno, T. Ida and S. Tanabe, Springer Proc. Phys., 2(EXAFS Near Edge Struct. 3) (1984) 206.
229. Y.M. Sun, D.N. Belton and J.M. White, ACS Symp. Ser., 288(Catal. Charact. Sci.) (1985) 80.
230. Y. Iwasawa and H. Sato, Chem. Lett., (1985) 507.
231. E.S. Shpiro, B.B. Dyusenbiva, G.V. Antoshin, O.P. Tkachenko and Kh.M. Minachev, Kinet. Katal., 25 (1984) 1505.
232. E.S. Shpiro, B.B. Dyusenbina, G.V. Antoshin, O.P. Tkachenko and Kh.M. Minachev, Perv. Sov.-Indiisk. Seminar. po Kataliz na Temu: Kataliz i Progress v Khim. Tekhnol.

Novosibirsk, (1984) 151; from reference Zh. Khim., (1984) Abstr. No. 23B4200.
233. H.R. Sadeghi and V.E. Henrich, Appl. Surf. Sci., 19 (1984) 330.
234. J. Sanz, J.M. Rojo, P. Malet, G. Munuera, M.T. Blasco, J.C. Conesa and J. Soria, J. Phys. Chem., 89 (1985) 5427.
235. J. Sanz and J.M. Rojo, J. Phys. Chem., 89 (1985) 4974.
236. J.B. Miller, S.J. DeCanio, J.B. Michel and C. Dybowski, J. Phys. Chem., 89 (1985) 2592.
237. D.G. Richards, J.O.H. Newman, Proc.-Int. Conf. Coal Sci., (1983) 223.
238. H. Fujitsu, N. Ikeyama, Y. Shigaki and I. Mochida, Bull. Chem. Soc. Japan, 58 (1985) 1849.
239. H. Miessner, H. Orita, S. Naito and K. Tamaru, React. Kinet. Catal. Lett., 28 (1985) 295.
240. H. Miessner, S. Naito and K. Tamaru, J. Catal., 94 (1985) 300.
241. H. Orita, S. Naito and K. Tamaru, J. Phys. Chem., 84 (1985) 3066.
242. S.C. Chuang, J.G. Goodwin, Jr. and I. Wender, J. Catal., 92 (1985) 416.
243. S.C. Chuang, J.G. Goodwin, Jr. and I. Wender, J. Catal., 95 (1985) 435.
244. S.C. Chuang, J.G. Goodwin, Jr. and I. Wender, Prepr. Pap.-Am. Chem. Soc., Div. Fuel Chem., 29 (1984) 250.
245. T.M. Dukhovnaya, K.K. Dzhardamalieva, G.A. Kil'dibekova and D.V. Sokol'skii, Neftekhimiya, (1985) 21.
246. F. Solymosi, A. Erdohelyi and I. Tombacz, Appl. Catal., 14 (1985) 65.
247. Y. Tanaka and T. Iizuka, Aust. J. Chem., 38 (1985) 293.
248. C.H. Dai and S.D. Worley, Chem. Phys. Lett., 114 (1985) 286.
249. K. Yamaguti and S. Sato, J. Chem. Soc., Faraday Trans. 1, 81 (1985) 1237.
250. P. Marginean and A. Olariu, J. Catal., 95 (1985) 1.
251. R.T.K. Baker, J.J. Chludzinski and J.A. Dumesic, J. Catal., 93 (1985) 312.
252. M. Malinowski, R. Makowski and R. Muranyi, Bull. Pol. Acad. Sci., Chem., 32 (1984) 169.
253. G.A. Branitskii, S.N. Mal'chenko and D.I. Mychko, Tr. Tbilis. Un-Ta, 248 (1984) 13.
254. J.S. Curran, J. Domenech, N. Jaffrezic-Renault and R. Philippe, J. Phys. Chem., 89 (1985) 957.
255. S. Sato, J. Catal., 92 (1985) 11.
256. M.M. Kolosova, S.A. Simanova, E.N. Yurchenko, E.S. Boichinova and V.I. Kuznitsov, Zh. Neorg. Khim., 30 (1985) 1493.
257. H. Toyuki, M. Itami, K. Hotta and Y. Kawamoto, Nippon Kagaku Kaishi, (1984) 1363.
258. M.S. Spencer, J. Catal., 93 (1985) 216.
259. See reference 258, and references therein.
260. M.S. Spencer, Prepr.-Am. Chem. Soc., Div. Pet. Chem.,30 (1985) 157.
261. H. Brumberger, F. DeLaglio, J. Goodisman, M.G. Phillips, J.A. Schwarz and P. Sen, J. Catal., 92 (1985) 199.
262. T.J. Lee and Y.G. Kin, Chem. Eng. Commun., 34 (1985) 277.
263. G.B. McVicker and J.J. Ziemiak, J. Catal., 95 (1985) 473.
264. M.A. Vannice, L.C. Hasselbring and B. Sen, J. Phys. Chem., 84 (1985) 2972.
265. M.A. Vannice, P. Odier, M. Bujor, J.J. Fripiat, ACS Symp. Ser., 288(Catal. Charact. Sci.) (1985) 98.

266. Y. Chen, H. Liu, H. Cai and B. Xie, Cuihua Xuebao, 5 (1984) 253.
267. K. Uosaki, R. Yoneda and H. Kita, J. Phys. Chem., 89 (1985) 4042.
268. R. Pollack, A.N. Bain and J.F. Houlihan, Altern. Energy Sources, [Proc. Miami Int. Conf.], 6th, 1983, 3 (Pub. 1985) 527.
269. C.M. Greenlief, J.M. White, C.S. Ko and R.J. Gorte, J. Phys. Chem., 89 (1985) 5025.
270. C.S. Ko and R.J. Gorte, Surf. Sci., 155 (1985) 296.
271. Y. Nosaka, Y. Ishizuka, K. Norimatsu and H. Miyama, Bull. Chem. Soc. Japan, 57 (1984) 3066.
272. B. Ohtani, H. Isaki, S. Nishimoto and T. Kagiya, Chem. Lett., (1985) 1075.
273. J. Cunningham and G.H. Al Sayyed, Nouv. J. Chim., 8 (1984) 469.
274. K. Kunimori, S. Matsui and T. Uchijima, Chem. Lett., (1985) 359.
275. D.E. Damiani and J.B. Butt, J. Catal., 94 (1985) 218.
276. H. Lin, Y. Chen, Y. Dong and H. Liu, Cuihua Xuebao, 5 (1984) 259.
277. V.M. Kolchanova and E.P. Mikheeva, React. Kinet. Catal. Lett., 26 (1984) 15.
278. D.N. Furlong, D. Wells and W. SAsse, J. Phys. Chem., 89 (1985) 626.
279. D.N. Furlong, D. Wells and W.H.F. Sasse, J. Phys. Chem., 89 (1985) 1922.
280. L. Loy and E.E. Wolf, Sol. Energy, 34 (1985) 455.
281. B. Hubesch and B. Mahieu, Polyhedron, 4 (1985) 669.
282. T. Nakahira and M. Graetzel, Makromol. Chem., Rapid Commun., 6 (1985) 341.
283. I.A. Ichou, M. Formenti and S.J. Teichner, Stud. Surf. Sci. Catal., 19(Catal. Energy Scene) (1984) 297.
284. E.A. Strel'tsov, D.V. Sviridov and A.I. Kulak, Elektrokhimiya, 20 (1984) 1671.
285. A.K. Rakhmanov, N.I. Kuntsevich and B.I. Shapiro, Zh. Nauchn. Prikl. Fotogr. Kinematogr., 30 (1985) 166.
286. Y. Saitoh, K. Ikeda, H. Ohbayashi, T. Nomura and K. Yokoyama, Nippon Kagaku Kaishi, (1985) 163.
287. J.A. Lercher, H. Vinek, H. Noller and J. Stoch, Appl. Catal., 12 (1984) 293.
288. J.A. Lercher, H. Vinek, S. Astegger, H. Noller and J. Stoch, Actas Simp. Iberoam. Catal., 9th, 1 (1984) 329.
289. H. Demiryont, Appl. Opt., 24 (1985) 2647.
290. H. Tsubomura, Y. Nakato, M. Hiramoto and H. Yano, Can. J. Chem., 63 (1985) 1759.
291. A.I. Kulak and S.K. Poznyak, Poverkhnost, (1985) 85.
292. D. Avnir, V.R. Kaufman and R. Reisfeld, J. Non-Cryst. Solids, 74 (1985) 395.
293. G. Seo, S. Kwon and H. Park, Hwahak Konghak, 22 (1984) 141.
294. G. Seo, S. Kwon, G. Lim and C. Cho, Hwahak Konghak, 22 (1984) 161.
295. M.A. Koshevnik, E.N. German and E.M. Guseinov, Deposited Doc., (1984) VINITI 5036-84, 123.
296. V.A. Polyboyarov, V.F. Anufrienko, N.G. Kalinina and S.V. Vosel, Kinet. Katal., 26 (1985) 751.
297. M. Anpo, N. Aikawa, Y. Kubokawa, M. Che, C. Louis and E. Giamello, J. Phys. Chem., 89 (1985) 5017.
298. M. Pickering, J. Chem. Ed., 62 (1985) 442.

299. J. Eicher, P. Klingelhoefer, U. Mueller and K. Dehnicke, Z. Anorg. Allg. Chem., 514 (1984) 79.
300. S.Ya. Kuchmii, S.V. Kulik, A.V. Korzhak and A.I. Kryukov, Teor. Eksp. Khim., 21 (1985) 560.
301. M.P. Pazos-Perez, M.E. Garcia-Fernandez, E. Freijanes, M. Gayoso, J.S. Casas and J. Sordo, An. Quim., Ser. B, 81 (1985) 7.
302. S. Zhang, L. Lai, M. Shao and Y. Tang, Wuli Huaxue Xuebao, 1 (1985) 335.
303. K. Wieghardt, D. Ventur, Y.H. Tsai and C. Krueger, Inorg. Chim. Acta, 99 (1985) L25.
304. G. Dessy, V. Fares, A. Flamini and A.M. Giuliani, Angew. Chem., 97 (1985) 433.
305. I.G. Ibadov, Sintez i Svoistva neorgan. Soedin., Baku, (1984) 110; from reference Zh. Khim., (L985) Abstr. No. 11V58.
306. R. Guilard and C. Lecomte, Coord. Chem. Rev., 65 (1985) 87.
307. P. Friant, J. Goulon, J. Fischer, L. Ricard, M. Schappacher, R. Weiss and M. Momenteau, Nouv. J. Chim., 9 (1985) 33.
308. I.V. Surov, A.S. Akopov and B.D. Berezin, Izv. Vyssh. Uchebn. Zaved., Khim. Khim. Tekhnol., 27 (1984) 880.
309. U. Mueller, P. Klingelhoefer, J. Eicher and R. Bohrer, Z. Kristallogr., 168 (1984) 121.
310. A.D. Garnovskii, I.S. Vasil'chenko, S.G. Kochin, L.S. Minkina, V.D. Khavryuchenko and L.E. Nivoroshkin, Koord. Khim., 11 (1985) 1156.
311. J. Uttamchandani and R.N. Kapoor, Indian J. Chem., Sect. A, 24A (1985) 242.
312. M. Caron and K.B. Sharpless, J. Org. Chem., 50 (1985) 1557.
313. J.M. Chong and K.B. Sharpless, J. Org. Chem., 50 (1985) 1560.
314. R. Hofer, D. Evard and A. Jacot-Guillarmod, Helv. Chim. Acta, 68 (1985) 969.
315. F. DiFuria, G. Modena and R. Seraglia, Synthesis, (1984) 325.
316. D. Seebach and M.A. Brook, Helv. Chim. Acta, 68 (1985) 319.
317. G.I. Dzhardimalieva, A.D. Pomogailo and A.N. Shupnik, Izv. Akad. Nauk SSSR, Ser. Khim., (1985) 451.
318. T. Shinoda, N. Shima and M. Tsukada, Surf. Sci., 163 (1985) 121.
319. G.A. Chubarov, S.M. Danov,and V.I. Logutov, Neftekhimiya, (1985) 129.
320. S.C. Goel, Synth. React. Inorg. Met.Org. Chem., 15 (1985) 533.
321. S.C. Chaudhry and J. Gupta, Indian J. Chem., Sect. A, 24A (1985) 150.
322. R.A. Jones, J.G. Hefner and T.C. Wright, Polyhedron, 3 (1984) 1121.
323. K. Szczegot, W. Nowy-Wiechula, M. Nowakowska, L. Studencki and I. Michalik, Zesz. Nauk.-Wyzsza Szk. Pedagog. im Powstancow Slask. Opolu, [Ser.]: Chem., 6 (1984) 101.
324. W. Sun and Y. Ren, Dalian Gongzueyuan Xuebao, 23 (1984) 138.
325. H. Kido, Ariake Kogyo Koto Senmon Gakko Kiyo, 21 (1985) 67.
326. X. Wan and Q. Luo, Shiyou Huagong, 14 (1985) 75.
327. V.A. Poluboyarov, P.M. Nedorezova, V.F. Anufrienko, F.S. Dyachkovskii, V.I. Tsvetkova and V.A. Zakharov, React. Kinet. Catal. Lett., 26 (1984) 245.

328. A.T. Prokof'ev, Z.K. Kasymbekova, N.N. Bubnov, S.P. Solodovnikov, M.E. Ignatov, E.G. Il'in and M.I. Kabachnik, Izv. Akad. Nauk SSSR, Ser. Khim., (1984) 2002.
329. H. Ogino, Kagaku (Kyoto), 40 (1985) 278.
330. Y. Sasaki, M.A. Everhart and J.E. Earley, Polyhedron, 4 (1985) 317.
331. A. Rodriguez, A. Sousa, M. Gayoso, R. Bastida and J. Romero, An. Quim., Ser. B, 79 (1983) 165.
332. W. Jabs and W. Gaube, Z. Anorg. Allg. Chem., 514 (1984) 179.
333. M.C. Martinez, M.T. Pereira, M.R. Bermejo and M. Gayoso, Acta Cient. Compostelana, 20 (1983) 75.
334. M.C. Martinez, M.T. Pereira, M.R. Bermejo and M. Gayoso, Acta CIent. Compostelana, 20 (1983) 181.
335. R.I. Kureshy, N.H. Khan, S. Tabassum, S.J. Majid, S.S.A. Zaidi and K.S. Siddiqi, Indian J. Chem., Sect. A, 24A (1985) 784.